

Multi-center Assessment of CNN-Transformer with Belief Matching Loss for Patient-independent Seizure Detection in Scalp and Intracranial EEG

Wei Yan Peh^{1,2,3}, Prasanth Thangavel^{1,3}, Yuanyuan Yao⁴, John Thomas⁵, Yee Leng Tan⁶, and Justin Dauwels^{4,*}

¹Nanyang Technological University (NTU), Interdisciplinary Graduate School (IGS), Singapore 639798.

²NTU, School of Computer Science and Engineering (SCSE), Singapore 639798.

³NTU, School of Electrical and Electronic Engineering (EEE), Singapore 639798.

⁴Delft University of Technology (TU Delft), Department of Microelectronics, 2628 CD Delft, Netherlands.

⁵Montreal Neurological Institute (MNI), McGill University, Montreal, QC H3A 2B4, Canada.

⁶National Neuroscience Institute (NNI), Singapore 308433.

*Corresponding Author: J.H.G.Dauwels@tudelft.nl

ABSTRACT

Neurologists typically identify epileptic seizures from electroencephalograms (EEGs) by visual inspection. This process is often time-consuming, especially for EEG recordings that last several hours or even days. To expedite the process, a reliable, automated, and patient-independent seizure detector is essential. However, developing a patient-independent seizure detector is challenging as seizures exhibit diverse morphologies and characteristics across different patients and recording devices. In this study, we propose a patient-independent seizure detector to automatically detect seizures in both scalp EEG (sEEG) and intracranial EEG (iEEG). First, we deploy a convolutional neural network (CNN) with transformers (TRF) and belief matching (BM) loss to detect seizures in single-channel EEG segments (channel-level detection). Next, we extract regional features from the channel-level outputs to detect seizures in multi-channel EEG segments (segment-level detection). At last, we apply postprocessing filters to the segment-level outputs to determine the start and end points of seizures in multi-channel EEGs (EEG-level detection). We introduce the minimum overlap evaluation scoring (MOES) as an evaluation metric that accounts for minimum overlap between the detection and seizure, improving upon existing assessment metrics. We trained the seizure detector on the Temple University Hospital Seizure (TUH-SZ) sEEG dataset and evaluated it on five other independent sEEG and iEEG datasets. On the TUH-SZ dataset, the proposed patient-independent seizure detector achieves a sensitivity (SEN), precision (PRE), average and median false positive rate per hour (aFPR/h and mFPR/h), and median offset of 0.772, 0.429, 4.425, 0, and -2.125s, respectively. Across all four adult datasets (excluding neonatal and paediatric datasets), we obtained SEN of 0.617-1.00, PRE of 0.534-1.00, aFPR/h of 0.425-2.002, and mFPR/h of 0-1.003. Meanwhile, on neonatal and paediatric datasets, we obtained SEN of 0.227-0.678, PRE of 0.377-0.818, aFPR/h of 0.253-0.421, and mFPR/h of 0.118-0.223. The proposed seizure detector can reliably detect seizures in adult EEGs (to less extent in neonatal EEGs) and takes less than 15s for a 30 minutes EEG. Hence, this system could potentially aid the clinicians in reliably identifying seizures expeditiously, allocating more time for devising proper treatment.

Keywords: Patient-independent Seizure Detection, Transformer, Belief Matching, Electroencephalogram.

Introduction

Epilepsy is a brain disorder characterized by the manifestations of sudden unprovoked seizures¹. Seizures are diverse, and vary significantly across patients in etiology, severity, and symptoms². Seizures are characterized by the location they affect and how far they spread³. Most seizures last from 30 seconds to two minutes, where a seizure lasting longer than five minutes is a medical emergency⁴. Approximately 60% of seizures are convulsive, where the patient experiences uncontrolled shaking. Examples of such seizures are tonic-clonic seizures, which can develop slowly from focal seizures⁵. The remaining 40% of seizures are non-convulsive, such as absence seizures, where the patient experiences a brief and sudden lapse of consciousness⁶. Epilepsy is diagnosed when a patient experiences two or more recurring seizures of any types⁷. Around 1% of the world population is diagnosed with epilepsy⁸. Moreover, approximately 10% of the population will experience a seizure within their lifetime⁹. Overall, provoked and unprovoked seizures occur in about 3.5 and 4.2 per 10000 individuals annually, respectively⁸. After a

seizure episode, the likelihood of encountering another seizure event increases to about 50%, bringing the individual to a much greater risk of relapsing¹⁰.

To detect seizures, an electroencephalogram (EEG) can be utilized. An EEG measures the electrical activity in the brain via electrodes attached to the scalp⁸. Scalp EEG (sEEG) records the brain activity by surface electrodes, while intracranial EEG (iEEG) measures the electrical signals directly via implanted electrodes¹¹. sEEGs are primarily utilized for patient monitoring, while iEEGs help in surgery planning for epilepsy patients¹². However, visual inspection of EEGs can be time-consuming. In practice, only small fractions of the entire recordings are inspected¹³. There is a need for automated seizure detectors that can detect seizures reliably and quickly. Most progress has been made toward patient-specific detectors, as seizure morphologies and characteristics strongly vary across patients. Consequently, designing a seizure detector that can detect any type of seizure in any patient can be challenging due to the wide variety of seizure patterns. Nonetheless, such patient-independent seizure detectors would be tremendously helpful for clinicians. There are several commercial seizure detectors available in the market, such as Persyst¹⁴, Encevis¹⁵, and BESA¹⁵. However, these detectors do not generalize well across patients and different EEG datasets, and cannot be applied to both sEEGs and iEEGs^{16,17}.

In recent studies on automated seizure detection from EEG, the seizure detectors are validated mainly on two public seizure datasets: the Temple University Hospital seizure (TUH-SZ) dataset^{18–21} and the Children’s Hospital Boston Massachusetts Institute of Technology (CHB-MIT) dataset^{19,22–24}. In many studies, different seizure detectors are proposed, including (standard) machine learning models^{25,26}, convolutional neural networks (CNNs)^{18,21,22,24,27}, recurrent neural networks (RNNs)^{18,20}, long short-term memory (LSTM)^{28,29}, transformer^{30,31}, transfer learning models^{20,32–34}, and temporal graph convolutional networks (TGCNs)³⁵. The seizure detectors proposed in these studies are similar in architecture or implementation. Most detectors first divide the multi-channel EEG into short multi-channel segments and classify each segment as normal against seizure (segment-level detection). Lastly, they determine the start and end points of the seizures from the segment-level outputs. For most studies, the main innovation lies in the design of the segment-level seizure detector, where most studies propose increasingly deep and complex neural networks with millions of parameters^{30,35}.

However, computationally intensive models may not necessarily improve patient-independent seizure detection, due to the associated increased risk of overfitting. Furthermore, it is shown in the literature that seizure detectors trained on large datasets reported similar results to those trained on smaller datasets^{35,36}. Overall, we observed a fundamental bottleneck that limits the performance of the state-of-the-art patient-independent seizure detectors. To resolve the bottleneck, we require a fresh perspective on this problem. As we will explain in the following, we address certain drawbacks of the existing seizure detector design and resolve some of its weaknesses in this study.

First, most modern seizure detectors identify seizures from short multi-channel segments (segment-level detection) before using the resulting segment-level outputs to determine the start and end points of seizures in the full EEG (EEG-level detection). Since these detectors are trained on annotated multi-channel EEG segments, they can only handle a fixed number of EEG electrodes (e.g., 21). To apply those models to EEGs with a different number of electrodes (e.g., 32), the models need to be retrained on EEGs with that same number of electrodes. In practice, the number of electrodes may vary; consequently, this limitation is a severe impediment to clinical applications.

To overcome this limitation, we proposed a seizure detector that starts by detecting seizures in single-channel segments (channel-level detection). We evaluate three variations of CNN for the channel-level detector: CNN with softmax loss (CNN-SM), CNN with belief matching (BM) loss (CNN-BM), and a CNN cascaded with a transformer and BM loss (CNN-TRF-BM). The BM loss is used to improve confidence performance and to obtain a more accurate prediction. A model with good calibration behaviour has a distribution of the probability predicted similar to the actual distribution and behaviour of probability observed in training data. In other words, when the output of the system is near 0 or 1, the accuracy should be high. By contrast, when the output is near 0.5, the system seems less confident, and the accuracy is expected to be lower. Therefore, the more confident the system is in its predictions, the more accurate it is supposed to be. Furthermore, the transformer is deployed to extract long-range patterns across the signals, while CNNs typically can only capture short-range patterns. We assess the three CNN models to determine the best model for the channel-level seizure detector. While studies proposed seizure detectors that detect seizures at individual channels, these studies analyzed single-channel EEGs, rather than single-channel segments from multi-channel EEGs^{37–41}. Consequently, while they performed channel-level seizure detection, they did not conduct segment-level detection. This limitation can severely impact the seizure detector, as multi-channel EEGs yield more information regarding the topological map than single-channel EEG recordings. Additionally, most of these studies performed patient-specific seizure detection.

Second, in the next stage, the outputs from the channel-level detector are aggregated, and from those outputs, seizures are detected in multi-channel EEG segments (segment-level detection). Concretely, we group the outputs

into five brain regions and compute statistical features for each region, which can be done for an arbitrary number of electrodes as long as there are two or more electrodes inside each region. At last, leveraging the outputs of the segment-level seizure detector, the proposed system determines the start and end points of the seizures (if any). As the system starts by processing individual channels and grouping the outputs into regions, independently of the number of electrodes, the proposed seizure detector can be applied to EEGs with an arbitrary number of electrodes. Moreover, not only can it be applied to sEEG, the same system can also be applied to iEEG without retraining. In this study, we trained the proposed seizure detector on a large sEEG dataset (TUH-SZ dataset) and evaluated it on five independent sEEG and iEEG datasets. The independent datasets consist of patients from different age groups (neonatal, paediatric, and adult) and types (humans and dogs). In comparison, existing seizure detectors for sEEGs and iEEGs are often trained and analyzed separately, and are usually trained and tested on the same dataset^{30,42} (with a few exceptions, see^{43–45} for example).

Third, to measure the effectiveness of seizure detectors, an adequate evaluation metric is necessary. Such metrics score a detection from the automated system based on how much it overlaps with a manually annotated seizure(s), considered to be the ground truth. Unfortunately, most studies do not state what metric has been applied to assess the seizure detectors. Consequently, comparing different detectors proposed in the literature can be challenging, even when evaluated on the same dataset. Several evaluation metrics have been proposed in the literature, including the epoch-based sampling (EBS)⁴⁶, any-overlap (OVLP)⁴⁶, time-aligned event scoring (TAES)⁴⁶, and increased margin scoring (IMS)¹⁶. However, these metrics do not reflect real-world clinical requirements. Therefore, we introduce the minimum overlap evaluation scoring (MOES), which requires the detection from the automated system to have a minimum overlap duration of 10s and a minimum overlap of 30% with a ground truth seizure for it to be considered correct (true positive). In contrast, OVLP and TAES require a non-zero (e.g., 0.1%) and perfect (100%) overlap, respectively, which tends to under- or over-penalize the detector, respectively. By requiring a non-trivial overlap, albeit not necessarily a perfect overlap, the MOES metric has a more adequate level of tolerance for clinical practice.

In summary, this paper makes the following contributions:

1. The proposed seizure detection system starts by processing individual EEG channels, and aggregates the outputs at individual channels into several brain regions, independently of the number of electrodes. As a result, the proposed system can be applied to both sEEG and iEEG with an arbitrary number of electrodes.
2. We apply CNN with transformer for seizure detection. While CNNs can extract complex patterns from EEG signals, they are less suitable for extracting long-range patterns. A transformer resolves this limitation as it can identify long-range features. Transformers have rarely been explored for seizure detection from EEG (but see^{30,31}). However, applying transformers on individual channels had not been proposed before.
3. We utilize a belief matching (BM) loss to improve the calibration performance. Unfortunately, many existing classification algorithms are not optimized for obtaining accurate probabilities, and the predictions they produce may be miscalibrated. Having a proper calibration performance is critical for decision-making. Bayesian approaches are rarely applied in EEG analysis, as most studies favour the traditional softmax (SM) loss.
4. We train the proposed patient-independent seizure detector on one sEEG dataset, and test it on five independent sEEG and iEEG datasets. Seizure detectors are usually not assessed on multiple independent datasets, and especially not on sEEGs and iEEGs simultaneously. Moreover, we obtain promising results on datasets on various EEG types (human and dog EEG) and from various age groups (neonatal, pediatric, adult EEG). This suggests that the proposed seizure detector tends to overfit less and generalizes well across multiple datasets.
5. We introduce the minimum overlap evaluation scoring (MOES) to assess the performance of seizure detectors. In contrast to existing metrics, MOES metric requires a non-trivial but not necessarily perfect overlap between the detection and ground truth seizure(s) for the detection to be considered correct. Existing metrics are either too lenient or strict on the detection overlap criteria, resulting in overly optimistic or pessimistic evaluations.
6. We conduct a detailed literature review on patient-independent seizure detectors and benchmark the proposed patient-independent seizure detectors with several state-of-the-art approaches.

Results

Channel-level Seizure Detection

We performed single-channel (channel-level) seizure detection with three channel-level detectors: CNN with a softmax (SM) loss (CNN-SM), CNN with a belief matching (BM) loss (CNN-BM), and CNN with a transformer and a BM loss (CNN-TRF-BM). In this setting, each single-channel EEG segment is labelled as “normal” or “seizure”. We summarized the results in Table 1. The precision-recall (PR) curves can be found in Supplementary Figure 5.

On the TUH-SZ dataset, the proposed channel-level detectors achieve high balanced accuracy (BAC), sensitivity

(SEN), and specificity (SPE) across all window lengths. Moreover, the expected calibration error (ECE) improved for all window lengths (except for 3s) when the SM loss is replaced with the BM loss (CNN-SM against CNN-BM). However, the ECE is slightly larger for the CNN-TRF-BM model. The performance peaks at a window length of 20s for all three models. Overall, the CNN-TRF-BM model attained the best results, followed by the CNN-BM and the CNN-SM model. As the channel-level detector attains good detection accuracy on the TUH-SZ dataset, deploying it as the primary training dataset seems to be a promising option.

Next, we assessed the channel-level detector, trained on the TUH-SZ dataset, on the five EEG datasets: the Children’s Hospital Boston Massachusetts Institute of Technology (CHB-MIT) dataset, the Sleep Wake Epilepsy Center at ETH Zurich (SWEC-ETHZ) dataset, the Helsinki University Hospital (HUH) dataset, the International Epilepsy Electrophysiology Portal (IEEGP) dataset, and the Epilepsy iEEG Multicenter (EIM) dataset. The detectors achieve high BACs on the CHB-MIT, SWEC-ETHZ, and EIM datasets, but yield poor BACs on the HUH and IEEGP datasets. For those datasets, seizures have only been annotated on the level of segments instead of channels; therefore, it is impossible to assess the channel detector reliably. Without channel-level annotations, we must assume that all channels within a multi-channel segment contain seizures. However, this is unlikely as seizures sometimes only occur in certain regions. In particular, focal seizures occur only in one hemisphere or at a few electrodes. Consequently, channels that do not exhibit seizures may be mislabelled as “seizure”, leading to errors during training and testing. However, segment-level and EEG-level detection results are reliable for those datasets.

Segment-level Seizure Detection

Next, we performed multi-channel segment (segment-level) seizure detection using the outputs from the three channel-level detectors. The segment-level seizure detection results are displayed in Table 2. The precision-recall (PR) curves are displayed in Supplementary Figure 5. We evaluated the three models for segment-level seizure detection on the six sEEG/iEEG datasets.

On the TUH-SZ dataset, the proposed segment-level detectors achieve high BAC, SEN, and SPE across all window lengths, similarly to the channel-level results. However, the ECE reported at segment-level is much greater than the channel-level counterparts. This is anticipated as the segment-level detector model does not minimize ECE, and instead utilizes a traditional loss function. Similarly, the performance peaks at a window length of 20s. Again, the CNN-TRF-BM model outshines the other two models.

Next, we evaluated the pre-trained segment-level seizure detector, trained on the TUH-SZ dataset, on the other five sEEG and iEEG datasets. We obtained excellent performance on all the datasets at various window lengths, except for the HUH dataset. The segment-level detectors obtain high BACs on the IEEGP dataset, even when the channel-level results on this dataset are not satisfactory.

Overall, the performance peaks at different window lengths across the six datasets. This might be due to the discrepancy in seizure types, patient types, and patient age groups across the different datasets. Consequently, the seizure length annotated can be very different for each institution (see Supplementary Figure 3 and Supplementary Table 1). For instance, for datasets with many short seizures, one should deploy a window length of 3s as it can capture shorter seizures, while a window length of 20s would be suboptimal.

EEG-level Seizure Detection

Next, we applied a post-processing module to determine the start and end times of the seizures based on the outputs of the segment-level detector. We summarized the results for the six datasets in Table 3. We refer the reader to Supplementary Figure 5 for the precision-recall curves. The EEG-level performance is computed according to the minimum overlap evaluation scoring (MOES), as it is more suitable for clinical practice than existing metrics (see Supplementary materials). We also considered other existing evaluation metrics for comparison in Table 4.

On the TUH-SZ dataset, the CNN-TRF-BM model leads to the most promising results, followed by the CNN-BM and the CNN-SM model. The CNN-TRF-BM EEG-level seizure detector attained a high SEN of 0.772, a decent PRE of 0.429, an average FPR/h (aFPR/h) of 0.425, and a median FPR/h (mFPR/h) of 0, and a median offset of -2.125s. While the aFPR/h is high, the mFPR/h is extremely low. This implies that the aFPR/h is skewed by a small number of EEGs containing an exceptionally huge amount of false detection. While the SEN is similar across all three models, the CNN-TRF-BM model reported the best PRE, which is critical for clinical deployment.

Similarly, we evaluated the EEG-level seizure detectors on the five sEEG and iEEG datasets. The CNN models yield high SEN, decent PRE, and low aFPR/h and mFPR/h on the CHB-MIT, SWEC-ETHZ, and EIM datasets. Meanwhile, on the HUH and IEEGP datasets, the model achieves low SEN (0.254 and 0.450, respectively), high PRE (0.841 and 0.917, respectively), and low mFPR/h (0.347 and 0, respectively). The poorer results on the HUH dataset are in line with our expectations since it is a neonatal dataset. The morphology of neonatal seizures differs vastly from adult seizures. Since the model has been trained on adult sEEG, it struggles to detect seizures

Table 1. Channel-level seizure detection results for different CNN models across six EEG datasets.

Dataset	W	CNN-SM						CNN-BM						CNN-TRF-BM					
		ECE	ACC	BAC	SEN	SPE	F1	ECE	ACC	BAC	SEN	SPE	F1	ECE	ACC	BAC	SEN	SPE	F1
TUH-SZ sEEG Adult	3	0.043	0.824	0.832	0.808	0.855	0.827	0.046	0.837	0.842	0.827	0.856	0.839	0.052	0.824	0.832	0.773	0.89	0.826
	5	0.043	0.84	0.836	0.769	0.902	0.84	0.035	0.845	0.842	0.862	0.821	0.848	0.03	0.85	0.83	0.767	0.892	0.849
	10	0.044	0.815	0.826	0.809	0.844	0.821	0.021	0.848	0.844	0.78	0.908	0.848	0.056	0.772	0.76	0.868	0.653	0.758
	20	0.044	0.836	0.845	0.812	0.877	0.837	0.027	0.845	0.851	0.834	0.868	0.846	0.033	0.852	0.858	0.828	0.889	0.853
CHB-MIT sEEG Paediatric	3	0.259	0.617	0.756	0.569	0.942	0.649	0.269	0.568	0.74	0.51	0.97	0.601	0.25	0.582	0.747	0.528	0.966	0.617
	5	0.181	0.669	0.763	0.56	0.966	0.668	0.205	0.62	0.739	0.494	0.984	0.616	0.095	0.742	0.808	0.666	0.95	0.755
	10	0.126	0.786	0.816	0.743	0.889	0.79	0.137	0.724	0.782	0.635	0.928	0.733	0.205	0.663	0.748	0.515	0.981	0.649
	20	0.129	0.777	0.78	0.592	0.969	0.758	0.141	0.777	0.782	0.606	0.959	0.765	0.153	0.755	0.756	0.534	0.978	0.733
SWEC-ETHZ iEEG Adult	3	0.069	0.803	0.721	0.56	0.882	0.804	0.127	0.814	0.725	0.557	0.892	0.813	0.107	0.814	0.726	0.56	0.891	0.814
	5	0.066	0.828	0.718	0.502	0.935	0.819	0.108	0.834	0.723	0.514	0.933	0.826	0.097	0.798	0.73	0.614	0.847	0.805
	10	0.084	0.772	0.726	0.648	0.805	0.785	0.112	0.805	0.74	0.628	0.853	0.812	0.094	0.844	0.737	0.535	0.939	0.837
	20	0.074	0.837	0.781	0.615	0.914	0.836	0.099	0.827	0.777	0.635	0.89	0.83	0.12	0.863	0.79	0.594	0.953	0.857
HUH sEEG Neonatal	3	0.259	0.506	0.491	0.187	0.794	0.454	0.399	0.403	0.403	0.249	0.903	0.496	0.408	0.4	0.4	0.245	0.902	0.492
	5	0.28	0.532	0.511	0.12	0.902	0.445	0.481	0.354	0.354	0.168	0.957	0.423	0.377	0.427	0.427	0.289	0.879	0.526
	10	0.228	0.527	0.507	0.217	0.796	0.482	0.403	0.417	0.417	0.264	0.912	0.511	0.508	0.358	0.358	0.168	0.974	0.423
	20	0.271	0.574	0.534	0.131	0.937	0.485	0.457	0.385	0.385	0.211	0.952	0.464	0.527	0.343	0.343	0.145	0.986	0.403
IEEGP iEEG Adult	3	0.358	0.536	0.536	0.453	0.952	0.613	0.346	0.533	0.533	0.444	0.975	0.608	0.351	0.532	0.532	0.445	0.968	0.606
	5	0.417	0.512	0.512	0.416	0.991	0.578	0.398	0.502	0.502	0.404	0.993	0.567	0.317	0.553	0.553	0.473	0.95	0.626
	10	0.317	0.574	0.574	0.508	0.9	0.651	0.352	0.562	0.562	0.479	0.976	0.631	0.386	0.523	0.523	0.428	0.998	0.59
	20	0.465	0.531	0.531	0.438	0.995	0.592	0.406	0.546	0.546	0.458	0.985	0.614	0.433	0.505	0.505	0.407	0.999	0.561
EIM iEEG Adult	3	0.201	0.653	0.662	0.583	0.741	0.643	0.128	0.658	0.669	0.579	0.759	0.649	0.144	0.659	0.666	0.588	0.745	0.651
	5	0.205	0.65	0.684	0.52	0.848	0.633	0.135	0.652	0.687	0.518	0.855	0.638	0.154	0.66	0.653	0.626	0.679	0.653
	10	0.207	0.659	0.641	0.658	0.624	0.65	0.154	0.666	0.663	0.622	0.704	0.66	0.155	0.665	0.701	0.536	0.866	0.653
	20	0.221	0.671	0.703	0.57	0.835	0.662	0.15	0.674	0.695	0.594	0.796	0.669	0.139	0.667	0.716	0.541	0.89	0.658
Average (All)	3	0.198	0.657	0.666	0.527	0.861	0.665	0.219	0.636	0.652	0.528	0.893	0.668	0.219	0.635	0.651	0.523	0.894	0.668
	5	0.199	0.672	0.671	0.481	0.924	0.664	0.227	0.635	0.641	0.493	0.924	0.653	0.178	0.672	0.667	0.573	0.866	0.702
	10	0.168	0.689	0.682	0.597	0.81	0.697	0.197	0.67	0.668	0.568	0.88	0.699	0.234	0.638	0.638	0.508	0.902	0.652
	20	0.201	0.704	0.696	0.526	0.921	0.695	0.213	0.676	0.673	0.556	0.908	0.698	0.234	0.664	0.661	0.508	0.949	0.678

Table 2. Segment-level seizure detection results for different CNN models across six EEG datasets.

Dataset	W	CNN-SM						CNN-BM						CNN-TRF-BM					
		ECE	ACC	BAC	SEN	SPE	F1	ECE	ACC	BAC	SEN	SPE	F1	ECE	ACC	BAC	SEN	SPE	F1
TUH-SZ sEEG Adult	3	0.051	0.818	0.736	0.888	0.584	0.817	0.027	0.820	0.733	0.901	0.565	0.816	0.262	0.823	0.751	0.885	0.616	0.824
	5	0.036	0.804	0.779	0.856	0.702	0.804	0.033	0.810	0.789	0.856	0.722	0.811	0.248	0.814	0.794	0.856	0.732	0.815
	10	0.039	0.815	0.817	0.783	0.850	0.815	0.031	0.833	0.833	0.815	0.852	0.833	0.027	0.832	0.831	0.800	0.862	0.831
	20	0.268	0.833	0.823	0.766	0.881	0.833	0.031	0.841	0.829	0.771	0.888	0.841	0.251	0.856	0.846	0.795	0.897	0.855
CHB-MIT sEEG Paediatric	3	0.122	0.789	0.801	0.804	0.798	0.789	0.117	0.798	0.811	0.819	0.804	0.801	0.258	0.833	0.847	0.808	0.886	0.837
	5	0.105	0.814	0.824	0.762	0.887	0.808	0.126	0.811	0.816	0.700	0.932	0.808	0.256	0.822	0.824	0.715	0.932	0.819
	10	0.118	0.874	0.841	0.745	0.936	0.867	0.100	0.875	0.831	0.686	0.976	0.862	0.104	0.879	0.837	0.698	0.976	0.866
	20	0.362	0.921	0.838	0.699	0.976	0.910	0.104	0.918	0.815	0.650	0.979	0.906	0.334	0.929	0.847	0.711	0.982	0.920
SWEC-ETHZ iEEG Adult	3	0.585	0.335	0.546	0.981	0.110	0.267	0.532	0.769	0.776	0.808	0.680	0.821	0.278	0.415	0.579	0.959	0.199	0.358
	5	0.487	0.417	0.600	0.980	0.220	0.380	0.355	0.584	0.601	0.514	0.886	0.659	0.234	0.541	0.649	0.917	0.381	0.529
	10	0.231	0.717	0.763	0.871	0.655	0.731	0.131	0.455	0.472	0.311	0.992	0.509	0.196	0.751	0.768	0.841	0.695	0.766
	20	0.226	0.806	0.832	0.881	0.773	0.819	0.151	0.449	0.463	0.296	0.996	0.493	0.261	0.877	0.872	0.858	0.874	0.883
HUH sEEG Neonatal	3	0.193	0.514	0.510	0.514	0.507	0.534	0.130	0.776	0.776	0.746	0.926	0.803	0.259	0.614	0.614	0.577	0.735	0.710
	5	0.200	0.470	0.545	0.376	0.714	0.471	0.232	0.746	0.746	0.709	0.932	0.784	0.303	0.533	0.533	0.429	0.869	0.618
	10	0.353	0.407	0.575	0.192	0.957	0.349	0.366	0.651	0.651	0.581	1.000	0.695	0.467	0.455	0.455	0.292	0.984	0.514
	20	0.357	0.413	0.575	0.183	0.968	0.349	0.414	0.628	0.628	0.533	0.817	0.691	0.444	0.426	0.426	0.251	0.994	0.483
IEEGP iEEG Adult	3	0.289	0.753	0.753	0.727	0.884	0.787	0.308	0.636	0.535	0.952	0.118	0.542	0.376	0.720	0.720	0.769	0.474	0.760
	5	0.311	0.722	0.722	0.779	0.439	0.759	0.278	0.658	0.555	0.968	0.143	0.559	0.325	0.737	0.737	0.706	0.892	0.778
	10	0.306	0.692	0.692	0.631	1.000	0.738	0.326	0.726	0.679	0.808	0.551	0.697	0.334	0.670	0.670	0.604	1.000	0.712
	20	0.290	0.621	0.621	0.571	0.720	0.690	0.345	0.757	0.705	0.883	0.528	0.733	0.398	0.616	0.616	0.429	0.991	0.648
EIM iEEG Adult	3	0.292	0.650	0.553	0.953	0.152	0.556	0.180	0.372	0.545	0.939	0.150	0.310	0.201	0.631	0.505	0.999	0.010	0.495
	5	0.279	0.568	0.459	0.893	0.025	0.468	0.280	0.577	0.670	0.904	0.436	0.575	0.203	0.654	0.538	0.989	0.087	0.543
	10	0.262	0.654	0.568	0.909	0.227	0.586	0.224	0.841	0.809	0.785	0.832	0.849	0.218	0.715	0.646	0.926	0.366	0.655
	20	0.204	0.648	0.644	0.603	0.685	0.611	0.246	0.833	0.850	0.886	0.808	0.846	0.224	0.780	0.745	0.881	0.609	0.749
Average (All)	3	0.255	0.643	0.650	0.811	0.506	0.625	0.216	0.695	0.696	0.861	0.541	0.682	0.272	0.673	0.669	0.833	0.487	0.664
	5	0.236	0.633	0.655	0.774	0.498	0.615	0.217	0.698	0.696	0.775	0.675	0.699	0.262	0.684	0.679	0.769	0.649	0.684
	10	0.218	0.693	0.709	0.689	0.771													

in neonatal sEEGs. Meanwhile, the IEEGP dataset contains some dog iEEGs, which could have different seizure patterns from adult humans. However, we observed that the detection performance is comparable for human and dog EEGs. Nonetheless, the proposed detector detected some neonate and dog seizures with high PRE, which can be tremendously valuable.

We also determined the detection offset, defined as the average duration between the start time of the seizure and the start time of its corresponding detection. As seen from Table 3, this offset can be negative. A negative offset does not imply that the system can predict seizures in advance, as the EEG data is analyzed offline⁴⁷. Therefore, data from future time intervals are being considered to decide whether a particular EEG segment is ictal.

In Table 4, we compare results for the CNN-TRF-BM model for different evaluation metrics (IMS, OVLP, TAES, and MOES). IMS always leads to the best results, followed by OVLP, MOES, and TAES. The results for MOES are similar to OVLP and IMS, despite MOES having a more stringent condition. This implies that the proposed seizure detector detects most seizures with at least 10s overlap and with 30% overlap between the seizure and detection. The results for the TAES metric are the lowest: a slight drop in SEN, much lower PRE, and significantly higher aFPR/h and mFPR/h. While there are significant differences across the different performance metrics, the results obtained by MOES are the most appropriate (see Supplementary materials). The detection condition of MOES reflects more accurately to clinical requirements and does lead to overly optimistic or pessimistic results.

Finally, to determine the effectiveness of the CNN-TRF-BM-based EEG-level seizure detector (Figure 1), we plot the normalized histograms of the TP and FN of seizures detected sorted by event duration, together with the normalized histogram of SEN, PRE, and FPR/h computed from individual EEGs across the datasets. From Figure 1(a), it can be seen that it is easier to detect a long seizure than a short event. Figure 1(b) and 1(c) reveal that the SEN and PRE are high for most EEGs, with only a minority of the files having a poor detection rate. Lastly, Figure 1(d) confirms that the system does not make false detections in most EEGs, as the mFPR/h is 0. Taken together, these figures seem to suggest that the proposed seizure detector performs well across most EEGs.

In Table 5, we computed the SEN of short (<10s) and long (>10s) seizures across the six datasets for various window lengths. As the CHB-MIT and IEEGP datasets do not contain annotated short seizures, we could not compute the SEN for those datasets. We observe that a window length of 20s leads to drastic drops in SEN for shorter seizures. On the other hand, a shorter window (3s and 5s) can more reliably capture shorter seizures, at the cost of potentially higher FPR/h.

The proposed seizure detectors, specifically the CNN-TRF-BM-based model, can detect patient-independent seizures across various independent sEEG and iEEG datasets without retraining. It takes less than 15s computation time to detect seizures in a 30 minutes EEG. Therefore, the proposed detector can help reduce the time required to annotate seizures in EEGs in clinical settings. However, while the results are appealing for adult human EEG (and dog EEGs), there is room for improvement for neonatal EEG. One may need to perform additional tuning or retraining to achieve better performance for such cases.

Discussion

Comparison with Existing Patient-independent Seizure Detectors

To compare the proposed seizure detector to the state-of-the-art is challenging, as there is a lack of standardized evaluation metrics, datasets, or training and testing procedures for the problem of seizure detection. The datasets considered in the literature vary in terms of the following:

1. Patient: age group (neonate, pediatric, adult, elderly), type (human or animal), diversity (number of patients, age, gender, race, or ethnicity)
2. Clinical setting: in-patient or out-patient
3. EEG: recording device, type (sEEG or iEEG)
4. Data: quantity (number of EEGs, duration of the EEGs, number of EEG channels), quality (signal-to-noise (SNR) ratio and prevalence of artifacts in the EEG)
5. Annotation: number of annotators, experience of annotators, the granularity of the annotations (e.g., channel-level vs. segment-level annotations)
6. Use case: patient-specific versus patient-independent seizure detection.

It is especially critical to specify the use case. Patient-specific detectors would yield much better performance than their patient-independent counterparts, but cannot be deployed readily clinically. Therefore, comparing those two different types of detectors is meaningless. Consequently, we consider here studies that report results on

Table 3. EEG-level seizure detection results for different CNN models evaluated with MOES across six EEG datasets.

Dataset	W	CNN-SM					CNN-BM					CNN-Transformer-BM				
		SEN	PRE	aFPR/h	mFPR/h	Offset	SEN	PRE	aFPR/h	mFPR/h	Offset	SEN	PRE	aFPR/h	mFPR/h	Offset
TUH-SZ sEEG Adult	3	0.7	0.457	0.803	0	-4.125	0.713	0.49	0.479	0	-4.5	0.772	0.429	0.425	0	-2.125
	5	0.704	0.48	0.555	0	-4.5	0.701	0.491	0.413	0	-1.5	0.653	0.476	0.411	0	0.625
	10	0.719	0.495	0.466	0	-1	0.701	0.512	0.237	0	1.5	0.671	0.534	0.954	0	0.5
	20	0.707	0.467	0.679	0	6.25	0.708	0.49	0.468	0	6	0.655	0.52	1.037	0	2.875
CHB-MIT sEEG Pediatric	3	0.638	0.112	1.721	1.099	0.711	0.613	0.14	0.916	0.539	-2.763	0.7	0.181	1.095	0.616	0.053
	5	0.678	0.143	1.514	0.868	-4.474	0.568	0.235	0.600	0.158	2.947	0.571	0.292	0.541	0.224	1.605
	10	0.734	0.254	1.041	0.618	0.158	0.704	0.411	0.291	0.026	4.737	0.678	0.377	0.421	0.118	4.684
	20	0.803	0.194	1.224	0.592	6.842	0.741	0.244	0.884	0.368	5.237	0.769	0.383	0.445	0.145	1.474
SWEC-ETHZ iEEG Adult	3	0.743	0.758	2.316	1.415	10.781	0.933	0.865	1.286	0.469	-2.156	0.938	0.878	0.895	0.559	7.687
	5	0.938	0.949	0.362	0	3.781	0.923	0.752	2.854	2.391	0.312	0.933	0.834	1.784	1.127	4.906
	10	0.933	0.785	2.223	0.884	4.187	0.825	0.695	3.265	2.858	15.719	0.857	0.748	2.899	1.648	10.375
	20	0.878	0.711	3.897	3.601	14.937	0.911	0.744	2.764	1.259	16.531	0.849	0.727	3.010	2.205	12.5
HUH sEEG Neonatal	3	0.298	0.334	2.565	1.094	6	0.623	0.576	2.320	2.276	-3.52	0.515	0.522	2.874	2.843	-2.255
	5	0.328	0.372	2.413	0.849	4.25	0.314	0.505	1.977	1.933	3.892	0.253	0.649	0.678	0.623	5.098
	10	0.254	0.397	1.671	0.181	11.5	0.214	0.807	0.334	0.303	13.52	0.227	0.818	0.253	0.223	10.853
	20	0.276	0.473	1.340	0.186	14.25	0.283	0.686	0.708	0.674	16.333	0.254	0.841	0.374	0.347	15.245
IEEGP iEEG Adult	3	0.6	0.964	0.523	0	-19	0.583	0.958	0.500	0	-14.5	0.667	0.8	2.200	2	-19
	5	0.667	0.8	2.624	2	-17	0.583	0.906	1.595	0	-17	0.617	0.944	1.120	0	-17
	10	0.592	0.946	0.750	0	-12	0.45	0.678	5.596	7	-12	0.5	0.753	4.423	5	-12
	20	0.567	0.805	3.846	0	-2	0.542	0.906	1.500	0	-2	0.45	0.917	0.500	0	-2
EIM iEEG Adult	3	0.972	1	0	0	-22.083	0.792	0.904	1.245	1.286	-7	1	1	1.523	0	-32.083
	5	0.979	0.938	1.080	0	-30.083	1	0.972	0.484	0.452	-15.417	1	1	0.647	0	-23.958
	10	1	1	0	0	-23.417	0.931	0.979	0.520	0	10.542	0.931	1	0.830	0	-1.333
	20	0.875	0.964	0.494	0.711	5.208	1	1	0	0	-0.792	0.951	1	0.507	0	-3.125
Average (All)	3	0.658	0.604	1.655	0.601	-4.619	0.71	0.655	1.458	0.762	-5.74	0.765	0.635	2.002	1.003	-7.954
	5	0.716	0.614	1.758	0.62	-8.004	0.682	0.643	1.654	0.822	-4.461	0.671	0.699	1.197	0.329	-4.787
	10	0.705	0.646	1.359	0.281	-3.429	0.637	0.68	2.041	1.698	5.67	0.644	0.705	1.797	1.165	2.18
	20	0.684	0.602	2.247	0.848	7.581	0.697	0.678	1.387	0.384	6.885	0.655	0.731	1.146	0.45	4.495

Table 4. EEG-level seizure detection results by the CNN-TRF-BM-based EEG-level detector evaluated with IMS, OVLP, TAES, and MOES across six EEG datasets.

Dataset	W	IMS					OVLP					TAES					MOES				
		SEN	PRE	aFPR/h	mFPR/h	Offset	SEN	PRE	aFPR/h	mFPR/h	Offset	SEN	PRE	aFPR/h	mFPR/h	Offset	SEN	PRE	aFPR/h	mFPR/h	Offset
TUH-SZ sEEG Adult	3	0.797	0.437	0.412	0	-7.5	0.775	0.43	0.423	0	-2	0.752	0.396	0.804	0.112	-2	0.772	0.429	0.425	0	-2.125
	5	0.694	0.494	0.378	0	-4.75	0.659	0.478	0.408	0	0.5	0.652	0.42	1.001	0	0.625	0.653	0.476	0.411	0	0.625
	10	0.658	0.588	0.562	0	-2.75	0.656	0.546	0.823	0	0.5	0.66	0.435	1.840	0	-1.5	0.671	0.534	0.954	0	0.5
	20	0.682	0.554	0.853	0	-2.25	0.667	0.526	1.026	0	3	0.658	0.358	2.902	0	3.5	0.655	0.52	1.037	0	2.875
CHB-MIT sEEG Pediatric	3	0.721	0.185	1.091	0.616	-5.921	0.7	0.181	1.095	0.616	0.053	0.622	0.151	1.126	0.622	0.053	0.7	0.181	1.095	0.616	0.053
	5	0.571	0.292	0.541	0.224	-4.395	0.571	0.292	0.541	0.224	1.605	0.52	0.255	0.667	0.336	2.842	0.571	0.292	0.541	0.224	1.605
	10	0.672	0.434	0.244	0.053	0.789	0.668	0.402	0.359	0.118	4.895	0.567	0.179	0.780	0.414	1.237	0.678	0.377	0.421	0.118	4.684
	20	0.762	0.396	0.391	0.092	-4.368	0.769	0.383	0.445	0.145	1.474	0.597	0.14	1.272	0.623	0.921	0.769	0.383	0.445	0.145	1.474
SWEC-ETHZ iEEG Adult	3	0.938	0.878	0.895	0.559	1.688	0.938	0.878	0.895	0.559	7.687	0.932	0.517	6.379	6.147	7.687	0.938	0.878	0.895	0.559	7.687
	5	0.933	0.853	1.620	1.127	-1.094	0.933	0.84	1.729	1.127	4.906	0.913	0.523	6.863	6.259	5.187	0.933	0.834	1.784	1.127	4.906
	10	0.86	0.805	2.424	1.327	11.219	0.857	0.755	2.667	1.618	10.656	0.896	0.55	6.168	5.717	6.156	0.857	0.748	2.899	1.648	10.375
	20	0.872	0.775	2.435	1.681	8.094	0.858	0.735	2.937	1.716	13.906	0.767	0.5	7.237	7.482	11.094	0.849	0.727	3.010	2.205	12.5
HUH sEEG Neonatal	3	0.563	0.554	2.756	2.725	0.402	0.544	0.539	2.795	2.76	-1.912	0.45	0.468	3.183	3.147	-1.912	0.515	0.522	2.874	2.843	-2.255
	5	0.284	0.662	1.620	0.6	7.765	0.254	0.649	0.678	0.623	5.059	0.203	0.546	1.237	1.186	4.431	0.253	0.649	0.678	0.623	5.098
	10	0.203	0.918	0.053	0.041	14.392	0.215	0.822	0.228	0.203	10.186	0.18	0.564	0.628	0.593	7.843	0.227	0.818	0.253	0.223	10.853
	20	0.278	0.865	0.315	0.295	17.059	0.271	0.845	0.374	0.347	16.765	0.173	0.518	1.088	1.057	18.167	0.254	0.841	0.374	0.347	15.245
IEEGP iEEG Adult	3	0.667	0.8	2.200	2	-37	0.667	0.8	2.200	2	-19	0.656	0.466	15.182	15.725	-19	0.667	0.8	2.200	2	-19
	5	0.65	1	0.000	0	-35	0.625	0.958	0.750	0	-17	0.592	0.547	13.431	13.571	-17	0.617	0.944	1.120	0	-17
	10	0.55	0.822	3.096	2	-29	0.5	0.777	3.173	0	-12	0.526	0.531	12.339	13.205	-12	0.5	0.753	4.423	5	-12
	20	0.467	1	0.000	0	-20	0.458	0.958	0.250	0	-2	0.36	0.374	15.284	16.997	-2	0.45	0.917	0.500	0	-2
EIM iEEG Adult	3	1	1	0.000	0	-41.083	1	1	0.000	0	-32.083	1	0.646	8.380	8.613	-32.083	1	1	1.523	0	-32.083
	5	1	1	0.000	0	-32.958	1	1	0.000	0	-23.958	0.992	0.662	7.811	8.218	-23.958	1	1	0.647	0	-23.958
	10	0.931	1	0.000	0	0.333	0.931	1	0.000	0	-1.333	0.975	0.681	7.071	7.547	-15.5	0.931	1	0.830	0	-1.333
	20	0.951	1	0.000	0	-12.125	0.951	1	0.000	0	-3.125	0.92	0.678	6.603	6.577	-0.208	0.951	1	0.507	0	-3.125
Average (All)	3	0.781	0.642	1.726	0.983	-14.902	0.771	0.638	1.735	0.989	-7.876	0.736	0.441	6.342	5.728	-7.876	0.765	0.635	1.802	1.003	-7.954
	5	0.689	0.717	0.866	0.325	-11.739	0.674	0.703	1.018	0.329	-4.815	0.645	0.492	5.502	4.928	-4.646	0.671	0.699	0.897	0.329	-4.787
	10	0.646	0.761	1.230	0.57	-0.836	0.638	0.717	1.375	0.323	2.151	0.634	0.49	4.971	4.579	-2.294	0.644	0.705	1.597	1.165	2.18
	20	0.669	0.765	0.832	0.345	-2.265	0.662	0.741	1.005	0.368	5.003	0.579	0.428	5.898	5.456	5.246	0.655	0.731	0.846	0.45	4.495

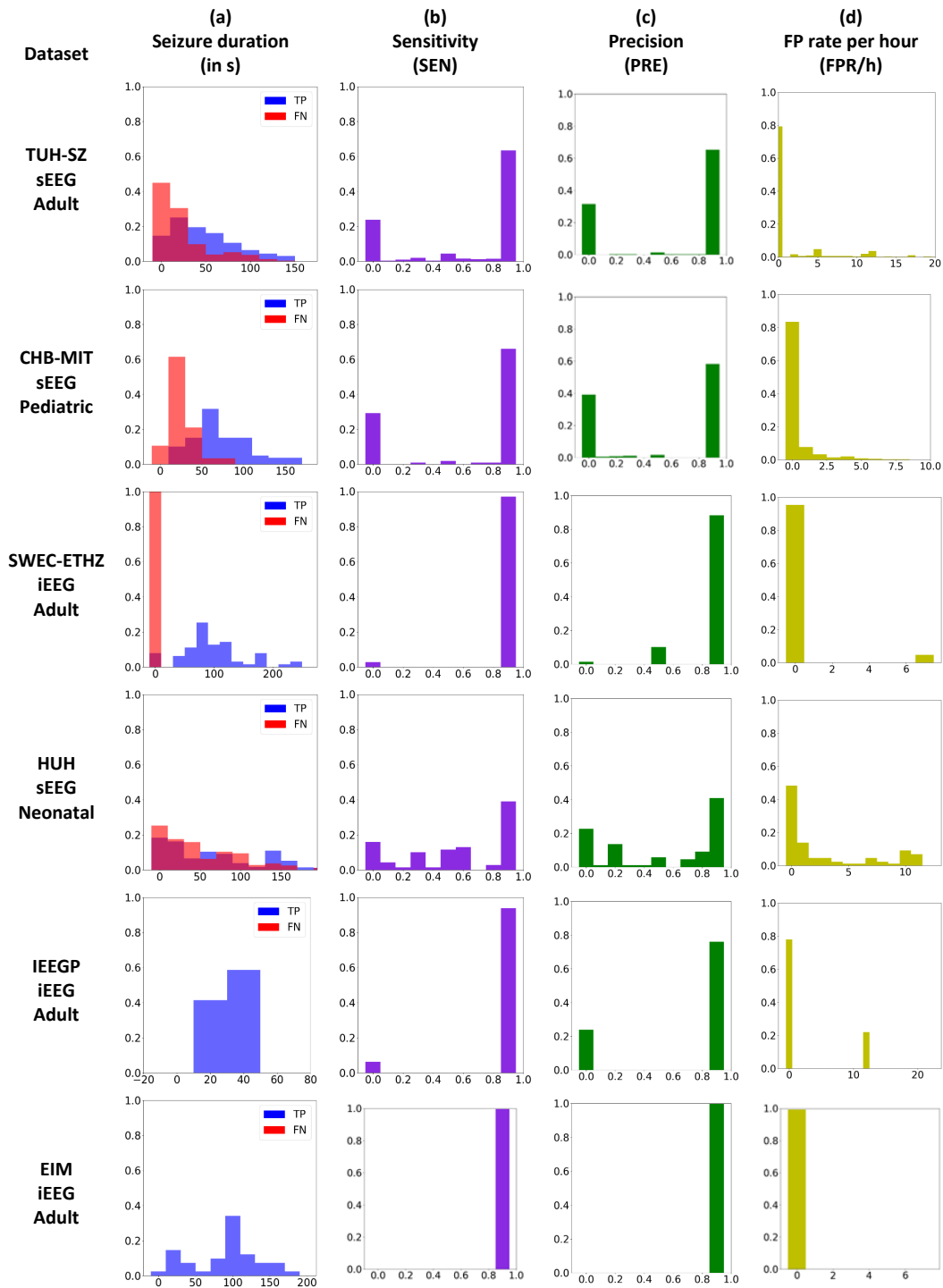


Figure 1. EEG-level seizure detection results for the CNN-TRF-BM model across different datasets. (a) normalized histograms of TPs and FNs sorted by seizure duration; (b-d) normalized histograms of the sensitivity (SEN), precision (PRE), and false positive rate per hour (FPR/h) for individual EEGs, respectively.

Table 5. SEN of short (<10s) and long (>10s) seizures detected by the CNN-TRF-BM-based model across the six datasets according to MOES metric.

Dataset	W	SEN		
		All SZ	Short SZ	Long SZ
TUH-SZ	3	0.772	0.532	0.797
	5	0.653	0.431	0.687
	10	0.671	0.343	0.72
	20	0.655	0.333	0.704
CHB-MIT	3	0.7	-	0.75
	5	0.571	-	0.631
	10	0.678	-	0.728
	20	0.769	-	0.819
SWEC-ETHZ	3	0.938	1	0.931
	5	0.933	1	0.926
	10	0.857	0	0.912
	20	0.849	0	0.868
HUH	3	0.515	0.818	0.496
	5	0.253	0.091	0.255
	10	0.227	0	0.248
	20	0.254	0	0.265
Neonatal	3	0.667	-	0.667
	5	0.617	-	0.617
	10	0.5	-	0.5
	20	0.45	-	0.45
IEEGP	3	1	1	1
	5	1	1	1
	10	0.931	0	0.955
	20	0.951	0	0.955

patient-independent seizure detection on the six datasets analyzed in this paper.

Seizure Detection on the TUH-SZ Dataset

Numerous patient-independent seizure detectors have been evaluated on the TUH-SZ dataset. Chatzichristos *et al.* designed an LTSM that achieved a SEN and FPR/h of 0.1237 and 0.06²⁰. Roy *et al.* utilized different machine learning models and reported a SEN and FPR/h of 0.916 and 137.311²¹. Meanwhile, Shah *et al.* applied an LTSM to detect seizures at segment-level and obtained SEN between 0.33-0.37 and FPR/h between 1.24-20.8¹⁸. Ayodele *et al.* trained a VGGNet and evaluated it on 24 EEGs, attaining a SEN, FPR/h, and offset of 0.7835, 0.9, and 2.32s, respectively¹⁹.

Most results reported are not suitable for clinical application; either the SEN of those detectors is too low, or the FPR/h is too high. Additionally, most studies did not report the seizure evaluation metrics. When they do, they utilize EBS and OVLP metrics, which fail to appropriately represent the requirements of a seizure detector. In contrast, the proposed CNN-TRF-BM seizure detector achieved superior results calculated with MOES (SEN, PRE, aFPR/h, and mFPR/h of 0.772, 0.429, 0.425, and 0, respectively), which is suitable for clinical applications. To the best of the author’s knowledge, no existing studies have reported the PRE, although it is an essential metric in clinical practice. Moreover, only few studies reported the offset.

Seizure Detection on the CHB-MIT Dataset

Similarly, many patient-independent detectors proposed in the literature have been assessed on the CHB-MIT dataset. Generally, seizure detectors evaluated in a patient-independent manner on the CHB-MIT dataset reported poor performance, especially for certain patients. More details can be found in the supplementary notes.

In the following, we briefly review the results of the CHB-MIT dataset reported in the literature. Furbass *et al.* deployed epileptiform wave sequence (EWS) analysis to classify seizure features and obtained a SEN and FPR/h of 0.67 and 0.32, respectively²². Gómez *et al.* applied a CNN classifier and achieved a SEN, SPE, and FPR/h of 0.531, 0.931, and 7.8, respectively²⁴. Ayodele *et al.* employed two datasets (CHB-MIT and TUH-SZ dataset) and reported a SEN, FPR/h, and offset of 0.7145, 0.76, and 2.32s, respectively¹⁹. Mansouri *et al.* trained their detector on the CHB-MIT (with five patients removed) and the TUH-SZ (only 24 patients) dataset, and evaluated the detector on the CHB-MIT dataset²³. They attained a SEN, SPE, and FPR/h of 0.83, 0.96, and 8, respectively²³. No studies reported the PRE nor offset.

The proposed CNN-TRF-BM model achieves better results on the CHB-MIT dataset, with SEN, PRE, aFPR/h, mFPR/h, and offset of 0.678, 0.377, 0.421, 0.118, and 4.684s, respectively. An important difference between our approach and the ones from the literature is that the proposed CNN-TRF-BM model is trained on the TUH-SZ dataset and tested on the CHB-MIT dataset. In contrast, the models from the literature are both trained and tested on the CHB-MIT dataset. The TUH-SZ dataset contains more seizures (3,055 events) compared to CHB-MIT (185

events), which may explain why the CNN-TRF-BM model outshines the state-of-the-art models. On the other hand, the training and test sets are different; therefore, it is not a priori clear that training on a larger but different dataset helps improve the performance. The numerical results show that the model generalizes well across the different datasets and can take advantage of the larger number of seizures in the TUH-SZ dataset for training purposes.

Seizure Detection on the SWEC-ETHZ Dataset

No existing seizure detectors had been evaluated on the SWEC-ETHZ dataset in a patient-independent manner. However, two existing studies performed seizure detection on the SWEC-ETHZ dataset in a patient-specific manner. Burrello *et al.* utilized hyperdimensional computing for EEG-level seizure detection and obtained a SEN and SPE of 0.960 and 0.948, respectively⁴⁸. Wang *et al.* trained a 1D CNN to detect seizures in multi-channel EEG segments and obtained a SEN, SPE, and ACC of 0.901, 0.998, and 0.997, respectively⁴². At the EEG-level, Wang *et al.* attained a SEN, FPR/h, and offset of 0.975, 0.07, and 13.2s. Overall, Wang *et al.* reported better results than Burrello *et al.*, while the results obtained by Wang *et al.* more similar to the ones reported in the current study. However, we reiterate that Wang *et al.* detected seizures in a patient-specific manner, which is expected to yield better performance than a patient-independent approach. It is interesting to note that Wang *et al.* also evaluated their seizure detector on both sEEGs (from CHB-MIT) and iEEGs (from SWEC-ETHZ). They found that the same seizure detector pipeline could be applied to both sEEG and iEEG. However, they trained and tested on the sEEG and iEEG separately; in other words, they did not test their model on an independent test set. In our study, we trained the model on one dataset (TUH-SZ dataset) and tested it on five independent EEG datasets.

Seizure Detection on the HUH Dataset

No seizure detectors have so far been evaluated on the HUH dataset in a patient-independent manner. Existing studies only evaluated patient-specific seizure detection. O’Shea *et al.* detected seizures at individual channels, achieving an AUC between 0.955-0.956⁴⁹. Similarly, Açıkoğlu *et al.* performed segment-level seizure detection and attained an ACC of 0.988. Consequently, the current study is the first to perform patient-independent seizure detection at EEG-level on the HUH dataset. Moreover, we applied a seizure detector trained on adult sEEGs to detect seizures in neonatal sEEGs, and attained promising results. The current study demonstrates that a seizure detector trained on adult seizures may capture neonatal seizures with a high PRE, despite the substantial age gap. We reiterate that the morphology of neonatal seizures differs vastly from adult seizures. As the model has been trained on adult sEEG, it struggles to detect seizures in neonatal sEEGs.

Seizure Detection on the IEEGP Dataset

Few studies investigated seizure detection on the IEEGP dataset. The biggest study on the IEEGP dataset is in the context of a competition on patient-specific seizure detection organized by the University of Pennsylvania and Mayo Clinic⁵⁰. This study is centred on segment-level detection in 1s segments rather than EEG-level seizure detection. The top 5 models achieved AUCs between 0.954 to 0.963. However, AUC is a poor metric for an imbalanced dataset, as seen in the IEEGP dataset where the non-ictal class outnumbers the ictal class 10 to 1. Meanwhile, Shen *et al.* performed patient-specific segment-level seizure detection on the IEEGP dataset and obtained accuracies between 0.59 to 0.79⁵¹. Similarly, accuracy is a poor metric for an imbalanced dataset. Therefore, the current study can be the baseline for patient-independent seizure detection on the IEEGP dataset.

Seizure Detection on the EIM Dataset

No earlier studies on automated seizure detection have been conducted on the EIM dataset. The existing studies aim to predict surgical outcomes (positive or negative)⁵². The current study is the first to analyze the EIM dataset for patient-independent seizure detection.

Comparison with Commercial Seizure Detectors

Several commercial seizure detectors are available in the market, such as Persyst¹⁴, Encevis¹⁵, and BESA¹⁵. Commercial seizure detectors can assist clinicians in reviewing EEG recordings, which may help to reduce time and boost the annotation accuracy⁵³. Earlier studies by Reus *et al.*¹⁶ and Koren *et al.*¹⁷ have compared the performance of Persyst, Encevis, and BESA. We summarized their findings against the performance of the proposed detector in Table 6. Reus *et al.* and Koren *et al.* evaluated the commercial seizure detectors on adult sEEG datasets; hence, we concentrate on the TUH-SZ dataset in this section.

Overall, the proposed model significantly outperforms the three commercial detectors in terms of higher SEN and lower FPR/h. The results for the proposed model are substantially better than for the three commercial systems in the study conducted by Reus *et al.* by a significant margin. The proposed system outperforms Persyst and BESA in the study by Koren *et al.*, with Encevis reporting similar results to the current study. However, we report results for

MOES, OVLP, and IMS metric, while Reus *et al.* and Koren *et al.* introduced an evaluation metric that seems to be more lenient. Indeed, Reus *et al.* consider a detection to be correct as long as the detection is within 30s before the start or after the end of the seizure. This approach is called the increased margin scoring (IMS) metric. Koren *et al.* implemented an altered version of IMS, where the margin is increased to 120s. These two evaluation metrics are less stringent than OVLP, as it allows lopsided detection by introducing a margin for error. Hence, if we were to compute the performance based on their metrics, we would report even better results (see Table 4).

Table 6. Performance of commercial seizure detectors against the proposed CNN-TRF-BM detector.

Author	Dataset	Number of Patients	Number of EEG	Number of Seizures	Duration (in hours)	Seizure Metrics	Seizure Detector	SEN	FPR/h	
									Average	Median
Reus <i>et al.</i> ¹⁶	Private	283	286	249	8771	IMS	Persyst 14	0.558	0.071	-
							Encevis 1.9.2	0.518	0.229	-
							BESA 2.0	0.430	0.100	-
Koren <i>et al.</i> ¹⁷	Private	81	-	790	6900	IMS	Persyst 13	0.816	0.9	-
							Encevis 1.7	0.778	0.2	-
							BESA 2.0	0.676	0.7	-
Current study	TUH-SZ	637	5610	3055	922.673	MOES	CNN-TRF-BM	0.772	0.425	0
						OVLP	CNN-TRF-BM	0.775	0.423	0
						IMS	CNN-TRF-BM	0.797	0.412	0

Transformer for Seizure Detection

We identified two studies that apply transformers for seizure detection^{30,31}. In other words, these systems studies did not implement a channel-level detector. Those systems do not analyze individual channels separately, but instead, only consider multi-channel EEG segments. The current study is the first to implement a channel-level seizure detector by means of transformers.

Bhattacharya *et al.* utilized a transformer for patient-specific seizure detection on the CHB-MIT and IEEGP dataset³⁰. For the CHB-MIT and IEEGP datasets, they attained an average SEN of 0.985 and 0.948, and FPR/h of 0.124 and 0, respectively. Overall, there are several differences in the study performed by Bhattacharya *et al.* as compared to the current study:

- We followed a patient-independent approach, while Bhattacharya *et al.* designed a patient-specific detector.
- The proposed system can detect seizures at individual channels, while the systems in Bhattacharya *et al.* can only detect seizures in multi-channel segments.
- We implemented BM loss to enhance generalization and calibration. Meanwhile, Bhattacharya *et al.* utilized the traditional SM loss.
- We performed seizure detection on all available EEGs. In contrast, Bhattacharya *et al.* cropped the EEGs to 30 minutes and discarded the remaining recordings. Consequently, they rejected a significant amount of EEG data from the CHB-MIT dataset, as all the EEGs in this dataset are at least 1 hour long.

As Bhattacharya *et al.* detected seizures in a patient-specific manner, it is not an appropriate benchmark for the models proposed in the current study. Nonetheless, we achieve decent SEN with low FPR/h on both datasets for patient-independent seizure detection. However, the results yielded from the IEEGP dataset were much poorer.

On the other hand, Pedoem *et al.* trained and evaluated a patient-independent transformer-based seizure detector on the TUH-SZ dataset³¹. They computed their EEG-level results according to three seizure evaluation metrics: EBS, OVLP, and TAES. Pedoem *et al.* attained the best results with OVLP metric, i.e., SEN and FPR/h of 0.09 and 1.301, respectively. However, their results are inferior to the ones achieved by the proposed CNN-TRF-BM model (SEN of 0.775, PRE of 0.43, aFPR/h of 0.423, and mFPR/h of 0, computed with OVLP). A possible explanation for the significant performance improvement could be the fact that the proposed systems detect, in the first stage, seizures at individual channels. Such spatial information might boost the accuracy of seizure detection.

Training the Seizure Detector on the TUH-SZ dataset Only

Patient-independent seizure detectors that do not require retraining or optimization can be readily deployed, which is convenient for clinical practice. In this study, we only trained the seizure detectors on the TUH-SZ dataset to replicate this scenario. By contrast, most existing studies utilize the same dataset for training and testing, and retrain a separate model for each dataset. Earlier, we showed that the proposed seizure detectors yield good performance on six EEG datasets. However, when testing on an independent dataset, we do not know whether the model trained on the TUH-SZ dataset would yield better performance than a model trained on the test dataset itself.

Table 7. Channel-, segment-, and EEG-level results trained and tested on the CHB-MIT dataset.

Dataset	Model	W	Channel-level						Segment-level						EEG-level				
			ECE	ACC	BAC	SEN	SPE	F1	ECE	ACC	BAC	SEN	SPE	F1	SEN	PRE	aFPR/h	mFPR/h	Offset
CHB-MIT Paediatric sEEG	1D CNN-SM	3	0.259	0.617	0.756	0.569	0.942	0.649	0.122	0.789	0.801	0.804	0.798	0.789	0.515	0.042	2.322	0.825	-16.875
		5	0.181	0.669	0.763	0.56	0.966	0.668	0.105	0.814	0.824	0.762	0.887	0.808	0.509	0.041	2.371	1.000	-15.750
		10	0.126	0.786	0.816	0.743	0.889	0.79	0.118	0.874	0.841	0.745	0.936	0.867	0.509	0.037	2.588	0.875	-15.750
CHB-MIT Paediatric sEEG	1D CNN-BM	3	0.269	0.568	0.74	0.51	0.97	0.601	0.117	0.798	0.811	0.819	0.804	0.801	0.510	0.044	2.221	0.750	-7.250
		5	0.205	0.62	0.739	0.494	0.984	0.616	0.126	0.811	0.816	0.700	0.932	0.808	0.516	0.028	3.420	0.881	3.500
		10	0.137	0.724	0.782	0.635	0.928	0.733	0.100	0.875	0.831	0.686	0.976	0.862	0.503	0.033	2.894	1.000	-7.000
CHB-MIT Paediatric sEEG	1D CNN-TRF-BM	3	0.141	0.777	0.782	0.606	0.959	0.765	0.104	0.918	0.815	0.650	0.979	0.906	0.515	0.033	2.947	1.000	-22.500
		5	0.25	0.582	0.747	0.528	0.966	0.617	0.258	0.833	0.847	0.808	0.886	0.837	0.577	0.214	0.101	0.000	9.750
		10	0.095	0.742	0.808	0.666	0.95	0.755	0.256	0.822	0.824	0.715	0.932	0.819	0.613	0.088	0.408	0.000	3.625
CHB-MIT Paediatric sEEG	1D CNN-TRF-BM	5	0.205	0.663	0.748	0.515	0.981	0.649	0.104	0.879	0.837	0.698	0.976	0.866	0.515	0.367	0.108	0.000	-3.375
		20	0.153	0.755	0.756	0.534	0.978	0.733	0.334	0.929	0.847	0.711	0.982	0.920	0.568	0.478	0.041	0.000	1.000

To address this question, we train and test the seizure detectors on the same dataset, i.e., the CHB-MIT dataset. We selected the CHB-MIT dataset as the total length of EEG in that dataset is comparable to the total duration of the TUH-SZ dataset (see Table 10). We report the channel-, segment-, and EEG-level results on the CHB-MIT dataset in Table 7 for the CNN-TRF-BM model trained on the TUH-SZ dataset. The CNN-TRF-BM model trained on the CHB-MIT dataset yields a SEN, PRE, aFPR/h and mFPR/h of 0.678, 0.377, 1.312, and 0.118, respectively. In comparison, the model trained on the TUH-SZ dataset yields a SEN, PRE, and median FPR/h of 0.678, 0.377, and 0.118 (see Table 3). While both models achieved similar FPR/h, the model trained on the TUH-SZ dataset attained vastly superior SEN and PRE.

This experiment suggests that training and evaluating a model with the same dataset might not necessarily generate the best results. Here, the detector trained on the TUH-SZ dataset performed much better than the model trained on the CHB-MIT dataset when tested on the CHB-MIT dataset. This can be due to the TUH-SZ dataset containing more seizures (3,055 events) and also more variety in the types of seizures, allowing the detector to learn from a more diverse seizure dataset. In comparison, the CHB-MIT dataset only contains 185 seizure events, which is significantly fewer. This experiment also suggests that it is possible to design neural network-based patient-independent seizure detectors that generalize well across different datasets.

Using a seizure detector trained on one dataset and testing it on another had been performed in the past³³. Saab *et al.* trained the public TUH-SZ dataset and a private Stanford University dataset, trained their seizure detector on data from one dataset and tested it on another³³. However, they only evaluated their system in terms of classifying EEG segments as ictal vs. non-ictal, and did not identify the start and end points of seizures. Interestingly, they did not achieve better results with this approach. When evaluating on the TUH-SZ dataset, the model trained on the TUH-SZ and Stanford datasets yielded an AUC of 0.78 and 0.74, respectively. Similarly, when evaluating on the Stanford dataset, the model trained on the Stanford and TUH-SZ dataset yielded an AUC of 0.94 and 0.70, respectively. Their results seem to suggest that their proposed model is unable to generalize from one dataset to another one; the best results are obtained when the detector is trained and tested on the same EEG dataset. In contrast, we showed that it is possible to obtain better results on one dataset by leveraging data from another data source. This approach works particularly well when the test dataset contains few seizure events, limiting the data available for training. As we will explain in the next section, the models proposed in this paper contain a small number of parameters compared to the models proposed in Saab *et al.*, therefore, they are less prone to overfitting and are better able to generalize across datasets.

We learn from this experiment that training seizure detectors on a large, diverse, and well-annotated dataset is a practical and fruitful approach, as the detectors may generalize well to independent datasets. Furthermore, training seizure detectors on a large variety of seizures from a large number of patients may boost the robustness of the detectors, allowing them to be deployed effectively in clinical practice for EEG recordings on various EEG machines at hospitals across the globe.

Complexity of Deep Learning Models for Seizure Detection

As previously mentioned, most seizure detectors proposed in the literature deployed a similar pipeline. Most existing seizure detectors do not analyze EEG signals at individual channels; therefore, they cannot localize seizures at individual channels. Instead, they first process multi-channel EEG segments, then proceed to detect the start and end points of seizures in the EEG. The main innovation in those studies lies in improving the deep neural networks that classify the multi-channel EEG segments as ictal or normal. These deep neural networks typically contain numerous layers (often 10+) and millions of parameters. Such models require substantial computational power for training and testing. Moreover, such networks tend to overfit to specific datasets, leading to poor generalization

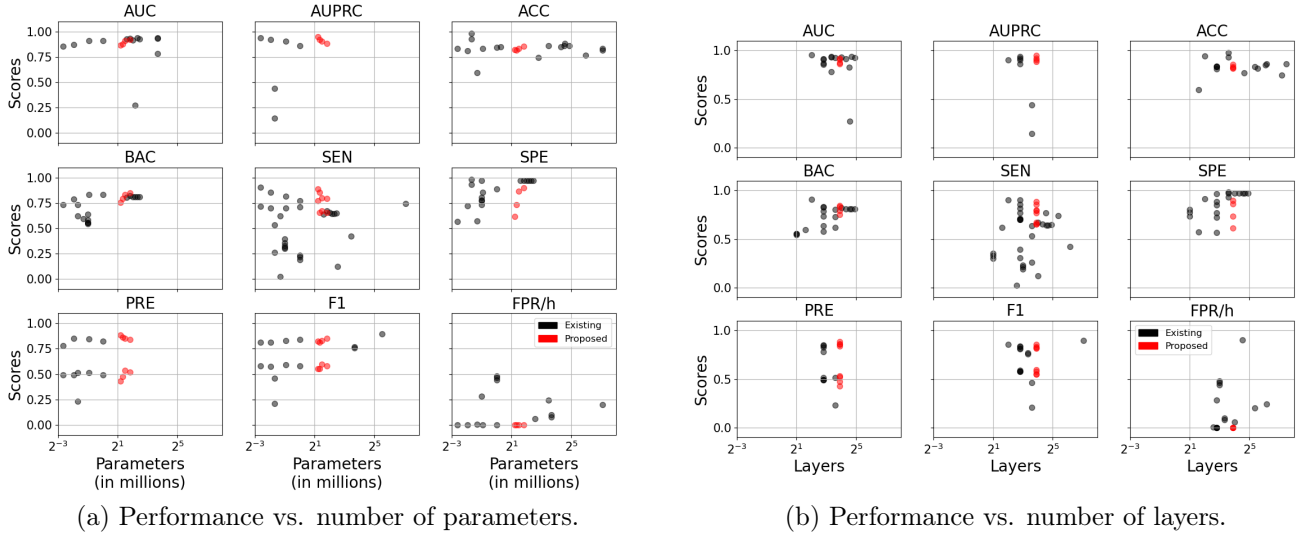


Figure 2. Performance of various seizure detectors as a function of (a) parameters (in millions) and (b) layers in the deep learning model. Each red indicates a model (all three models) deployed in the current study on the TUH-SZ dataset, while each black dot denotes a model in literature^{20,24,27–29,32–35,54–59}. In all the plots, the x-axis is in the logarithmic scale of base 2. We displayed all nine performance metrics, as studies tend to report different metrics, making comparison difficult.

capability. We explore whether deeper models lead to better seizure detection performance.

In Table 8, we list existing deep learning systems for seizure detection, and provide information about their design and performance. Existing neural networks for seizure detectors contain many layers, ranging between 2 and 709, and contain between 7,600 to 138 million parameters. The inputs to those models also vary significantly, ranging from 5,888 to 228,000 input data points. In contrast, the three proposed seizure detectors only require between 384 to 2,560 input data points, for window lengths varying from 5s to 20s. Moreover, the models contain 7 to 15 layers, with 0.16 to 3.5 million parameters for the CNN and CNN-TRF models. The input size, number of layers, and number of parameters for the proposed models are much smaller than for most of the existing models listed in Table 8.

Next, we examined the correlation between model size and performance for seizure detection. Due to the vast variability in the metrics reported by various studies, it is challenging to make a comparison. Hence, we plotted all nine metrics (AUC, AUPRC, ACC, BAC, SEN, SPE, PRE, F1, and FPR/h) versus the number of parameters (in millions) and the number of layers in the neural networks in Figure 2. Generally, AUC, BAC, AUPRC, SPE, and F1 scores are used in segment-level analysis, while the SEN, PRE, and FPR/h are used in EEG-level detection. The proposed seizure detector models reported higher SEN and lower FPR/h than most models with more parameters and layers. The AUC, ACC, BAC, and F1 were comparable, while the SPE was poorer in our model. However, SPE is only computed in segment-level classification, which is not an EEG-level detection metric. Moreover, the proposed models obtained better AUPRC, SEN, and FPR/h than most existing models with fewer parameters and layers. These studies deployed different metrics, not limited to EBS, IMS, OVLP, and TAES. Nevertheless, we only reported the results with MOES in Figure 2, as MOES is more appropriate as an evaluation metric. However, we can refer to Table 4 for results obtained from other metrics (EBS, IMS, OVLP, and TAES).

Overall, the proposed models outshine models with vastly more parameters. Therefore, this study suggests that designing ever-bigger neural networks for patient-independent seizure detection may not be a fruitful avenue for research. Instead, alternative pipelines with substantially fewer parameters may perform comparably to the state-of-the-art or even better. In this study, we demonstrated in particular that by first detecting seizures at individual channels, one can not only localize seizures at specific channels but also vastly reduce the number of parameters (to about 4 million in total) while achieving the same or increased level of performance.

Table 8. Comparison of the proposed seizure detector models to existing models from the literature in terms of complexity and detection performance.

Author	Model	Layers	Parameters (in millions)	Input Size	AUC	AUPRC	ACC	BAC	SEN	SPE	PRE	F1	FPR/h
Asif <i>et al.</i> ⁵⁴	SeizureNet	133	45.94	150,528	-	-	-	-	-	-	-	0.896	-
	AlexNet	25	62	51,529	-	-	0.768	-	-	-	-	-	-
Raghu <i>et al.</i> ³²	VGG16	41	138	50,176	-	-	0.833	-	-	-	-	-	-
	VGG19	47	138	50,176	-	-	0.818	-	-	-	-	-	-
	SqueezeNet	68	1.2	51,529	-	-	0.851	-	-	-	-	-	-
	GoogleNet	144	7	50,176	-	-	0.745	-	-	-	-	-	-
	Inceptionv3	316	24	89,401	-	-	0.883	-	-	-	-	-	-
	DenseNet201	709	20	50,176	-	-	0.851	-	-	-	-	-	-
	ResNet18	72	11	50,176	-	-	0.862	-	-	-	-	-	-
	ResNet50	177	23	50,176	-	-	0.862	-	-	-	-	-	-
	ResNet101	347	29.4	50,176	-	-	0.863	-	-	-	-	-	-
Covert <i>et al.</i> ³⁵	TGCN	30	5.5	415,107	0.926	-	-	0.809	0.648	0.970	-	-	-
	TGCN	26	5	415,107	0.935	-	-	0.808	0.645	0.970	-	-	-
	TGCN	24	4.5	415,107	0.270	-	-	0.808	0.645	0.970	-	-	-
	TGCN	20	4	415,107	0.917	-	-	0.812	0.653	0.970	-	-	-
	TGCN	16	3.5	415,107	0.931	-	-	0.820	0.669	0.970	-	-	-
	TGCN	12	3	415,107	0.928	-	-	0.803	0.635	0.970	-	-	-
Hossain <i>et al.</i> ⁵⁵	CNN	4	0.04	11,500	-	-	-	0.908	0.900	0.917	-	-	-
Yuan <i>et al.</i> ⁵⁶	CNN	4	0.04	17,664	0.957	0.906	0.944	-	-	-	-	0.853	-
Zhou <i>et al.</i> ⁵⁷	CNN	3	0.4	5,888	-	-	0.595	0.595	0.618	0.572	-	-	-
Saab <i>et al.</i> ³³	ChronoNet	10	12.7	45,600	0.930	-	-	-	-	-	-	0.770	0.100
Emami <i>et al.</i> ³⁴	VGG16	41	138	50,176	-	-	-	-	0.740	-	-	-	0.200
Ansari <i>et al.</i> ²⁷	CNN	23	0.0076	54,000	0.830	-	-	-	0.770	-	-	-	0.900
Khalkhali <i>et al.</i> ⁵⁸	ResNet	72	11	65,536	-	-	-	-	0.421	-	-	-	0.241
Shah <i>et al.</i> ⁵⁹	CNN-LSTM	7	0.5	77,440	-	-	-	0.638	0.308	0.969	-	-	0.281
	CNN-MLP	7	0.5	77,440	-	-	-	0.580	0.391	0.768	-	-	3.216
	IPCA-LSTM	2	0.5	77,440	-	-	-	0.553	0.330	0.776	-	-	3.063
	HMM-LSTM	2	0.5	77,440	-	-	-	0.553	0.301	0.805	-	-	2.538
	HMM-SdA	2	0.5	77,440	-	-	-	0.544	0.354	0.734	-	-	3.225
Gomez <i>et al.</i> ²⁴	CNN	12	0.314	21,504	-	0.440	0.929	0.731	0.531	0.931	0.514	0.461	7.800
Yang <i>et al.</i> ²⁸	CNN-LTSM	6	0.4	34,038	-	-	-	-	0.020	-	-	-	0.007
Thyagachandran <i>et al.</i> ²⁹	LTSM	8	1	194,560	-	-	-	-	0.189	-	-	-	0.481
Chatzichristos <i>et al.</i> ²⁰	U-Net	16	5.88	76,000	-	-	-	-	0.124	-	-	-	0.060
Current study	CNN	7	0.16	384	-	-	-	-	0.713	-	0.490	0.581	0
	CNN	7	0.26	640	-	-	-	-	0.701	-	0.491	0.578	0
	CNN	7	0.52	1,280	-	-	-	-	0.701	-	0.512	0.592	0
	CNN	7	1	2,560	-	-	-	-	0.708	-	0.490	0.579	0
Current study	CNN-TRF	15	2.3	384	-	-	-	-	0.772	-	0.429	0.552	0
	CNN-TRF	15	2.5	640	-	-	-	-	0.653	-	0.476	0.551	0
	CNN-TRF	15	2.8	1,280	-	-	-	-	0.671	-	0.534	0.595	0
	CNN-TRF	15	3.5	2,560	-	-	-	-	0.655	-	0.520	0.580	0

Benefits of Channel-level Seizure Detection

In this study, we proposed to detect seizures starting from single-channel segments (channel-level detection). However, many seizure detectors in the literature detect seizures directly from multi-channel segments (segment-level detection). This approach usually requires a fixed number of channels, an important limiting factor for clinical practice where the number of channels may vary depending on the EEG cap and machine. Moreover, the clinical setting may vary (inpatient vs. outpatient), while EEG caps for inpatient and outpatient recordings typically have a different number of electrodes. Moreover, this approach may have poor generalization performance, as the system might be strongly overfitted to a particular EEG electrode configuration and dataset. Here, we refer to seizure detector pipelines that detect seizures starting from single-channel segments as 1D models, while detectors that detect seizures starting from multi-channel segments as 2D models.

To further evaluate the benefits of the three proposed 1D seizure detectors, we designed two 2D seizure detectors that directly perform segment-level classification from the EEG signals. Those 2D models are identical to the 1D ones, except that the 1D convolutional filters are replaced with 2D filters. We optimized the 2D CNNs on the TUH SZ dataset with the SM and BM loss, leading to the two different 2D seizure detectors. As all the sEEGs in the TUH-SZ dataset contain 20 common channels, we fixed the number of channels to 20. Hence, the input of the 2D segment-level CNN models has dimension $(W * 128 * 20)$, where $W \in \{3, 5, 10, 20\}$ is the window length. Finally, we combined the 2D segment-level detectors with the same EEG-level pipeline to compute the EEG-level detections.

We trained and evaluated the 2D models on the TUH-SZ dataset for the segment- and EEG-level seizure detection. Next, we deployed the 2D models trained on the TUH-SZ dataset to detect seizures in the CHB-MIT dataset; in this way, we evaluate the generalizability of the model. We only consider the CHB-MIT dataset for the assessment, as it is the only dataset with EEGs with the same 20 common channels. Finally, we trained and evaluated the 2D models on the CHB-MIT dataset, and compared them to the models trained on the TUH-SZ dataset.

We display the segment- and EEG-level results for the TUH-SZ and CHB-MIT datasets in Table 9, where the EEG-level results are computed by the MOES metric. When trained and evaluated on the TUH-SZ dataset, the 2D models attain much weaker results for both segment- and EEG-level classification than the 1D models (see Table 3 for comparison). Those models also perform poorly on the CHB-MIT dataset, leading to substantially lower SEN and PRE scores than the 1D models. Moreover, when the 2D models were trained and evaluated on the CHB-MIT dataset, we obtained the worst results thus far, with PRE lower than 5% for all cases. These numerical results are in line with many 2D models reported in the literature^{20,28,29,57–59}.

Overall, 2D models underperform compared to the 1D models by a considerable margin. In conclusion, the channel-level detector appears to be vital for achieving superior generalization performance. Moreover, with the channel-level outputs, as seen in Supplementary Figure 6, we can identify the channels that exhibit the seizure by tracing the channels with the highest seizure probabilities. This would be impossible with a direct segment-level detection approach, as in the 2D models.

Table 9. Results of 2D seizure detectors on the TUH-SZ and CHB-MIT dataset.

Testing Dataset	Training Dataset	Model	W	Segment-level					EEG-level						
				ECE	ACC	BAC	SEN	SPE	F1	F1	SEN	PRE	aFPR/h	mFPR/h	Offset
TUH-SZ EEG Adult	TUH-SZ	2D CNN-SM	3	0.106	0.769	0.772	0.717	0.827	0.770	0.544	0.659	0.463	2.555	0	9.125
			5	0.119	0.791	0.769	0.672	0.866	0.788	0.538	0.674	0.448	2.764	0	7.000
			10	0.149	0.849	0.751	0.566	0.937	0.842	0.530	0.656	0.444	3.020	0	7.500
			20	0.160	0.859	0.734	0.534	0.933	0.854	0.510	0.521	0.499	1.741	0	3.250
TUH-SZ EEG Adult	TUH-SZ	2D CNN-BM	3	0.106	0.801	0.805	0.753	0.857	0.801	0.574	0.659	0.509	2.095	0	-5.250
			5	0.119	0.816	0.791	0.678	0.904	0.812	0.584	0.668	0.519	2.068	0	-7.875
			10	0.149	0.857	0.782	0.635	0.929	0.854	0.559	0.658	0.486	2.402	0	-3.750
			20	0.160	0.868	0.711	0.468	0.955	0.856	0.528	0.506	0.553	1.499	0	5.250
CHB-MIT Paediatric sEEG	CHB-MIT	2D CNN-SM	3	0.173	0.717	0.739	0.681	0.797	0.71	0.078	0.520	0.042	2.221	0.134	-16.875
			5	0.143	0.732	0.748	0.638	0.858	0.714	0.079	0.503	0.043	3.420	0.520	-17.250
			10	0.122	0.782	0.755	0.639	0.871	0.765	0.076	0.503	0.041	2.894	0.201	-16.000
			20	0.168	0.872	0.786	0.636	0.936	0.861	0.086	0.509	0.047	2.947	0.418	-16.250
CHB-MIT Paediatric sEEG	CHB-MIT	2D CNN-BM	3	0.165	0.716	0.732	0.687	0.776	0.707	0.082	0.510	0.044	2.221	0.750	-7.250
			5	0.145	0.733	0.748	0.655	0.841	0.716	0.061	0.505	0.032	2.951	0.769	-4.750
			10	0.112	0.779	0.75	0.633	0.868	0.759	0.063	0.508	0.034	2.892	1.023	-7.375
			20	0.16	0.868	0.783	0.635	0.932	0.858	0.067	0.510	0.036	2.692	0.848	-22.250
CHB-MIT Paediatric sEEG	TUH-SZ	2D CNN-SM	3	0.233	0.584	0.662	0.365	0.959	0.547	0.303	0.439	0.231	0.391	0.040	-2.737
			5	0.159	0.677	0.680	0.429	0.931	0.646	0.292	0.626	0.190	1.372	0.997	-4.658
			10	0.148	0.744	0.714	0.290	0.981	0.690	0.383	0.536	0.298	0.821	0.421	-2.447
			20	0.083	0.843	0.658	0.265	0.991	0.798	0.370	0.376	0.365	0.113	0.000	-5.184
CHB-MIT Paediatric sEEG	TUH-SZ	2D CNN-BM	3	0.357	0.515	0.613	0.239	0.987	0.451	0.426	0.368	0.505	0.129	0.000	1.526
			5	0.383	0.524	0.541	0.084	0.998	0.416	0.115	0.078	0.218	0.072	0.000	-0.395
			10	0.156	0.750	0.648	0.307	0.989	0.696	0.441	0.524	0.380	0.396	0.050	-0.737
			20	0.068	0.853	0.691	0.341	0.987	0.817	0.474	0.461	0.488	0.183	0.026	-8.526

Conclusion

This study proposed patient-independent seizure detectors that identify seizures on three EEG scales (see Supplementary Figure 1): single-channel EEG segments (channel-level detection), multi-channel EEG segments (segment-level detection), and entire EEGs (EEG-level detection). Firstly, the channel-level detectors detect seizures in single-channel segments through a CNN-based deep learning model (CNN-SM, CNN-BM, or CNN-TRF-BM). We perform channel-level detection at all channels of multi-channel EEG segments. Next, we extract statistical features from the channel-level outputs based on different scalp regions. Then, we apply a machine learning model to classify the segment-level features as normal or ictal. At last, we apply post-processing filters to the segment-level outputs to determine the start and end times of any detected seizures.

We trained and tested the proposed seizure detectors on the TUH-SZ sEEG dataset, before evaluating the pretrained detectors on five independent sEEG and iEEG datasets without retraining. We introduced a new metric named MOES to measure the EEG-level seizure detection performance, and compare it to existing metrics. MOES addresses some shortcomings of the latter. To the best of the author’s knowledge, this study is one of the first to incorporate a channel-level detector within the seizure detection system^{37–41}. Moreover, we implemented a pipeline that can detect seizures in both sEEGs and iEEGs with any number of electrodes. Furthermore, we demonstrated that a channel-level detector is essential for reliable seizure detection and boosting the generalization performance. Finally, the proposed seizure detector is computationally efficient, with a computation time of less than 15s for a 30 minutes EEG. Hence, the detector may help accelerate and improve EEG annotation in clinical practice.

In future work, we will address the problem of detecting artifacts before seizure detection⁶⁰. The artifact detector

will be designed to reduce FPR/h and improve PRE of the seizure detector. Consequently, it might be able to reject artifacts without eliminating important cerebral signals, such as slow waves, sharp waves, and seizures in EEGs.

Methods

Dataset

We analyze six public sEEG and iEEG datasets in this study:

1. Temple University Hospital Seizure (TUH-SZ) dataset⁶¹
2. Children’s Hospital Boston Massachusetts Institute of Technology (CHB-MIT) dataset⁶²
3. Sleep Wake Epilepsy Center at ETH Zurich (SWEC-ETHZ) dataset⁴⁸
4. Helsinki University Hospital (HUH) dataset⁶³
5. International Epilepsy Electrophysiology Portal (IEEGP) dataset⁶⁴
6. Epilepsy iEEG Multicenter (EIM) dataset⁵²

Table 10. Information on the six sEEG and iEEG datasets analyzed in the study.

Information	Details	TUH-SZ	CHB-MIT	SWEC-ETHZ	HUH	IEEGP	EIM
EEG Details	Patient Type	Human	Human	Human	Human	Human/Dog	Human
	Patient Age Group	Adult	Paediatric	Adult	Neonatal	Adult	Adult
	EEG Type	sEEG	sEEG	iEEG	sEEG	iEEG	iEEG
	F_s (Hz)	250-1000	256	512	256	400-5000	250-1000
	Channel Name	Available	Available	Unavailable	Available	Unavailable	Unavailable
	Channel-level Annotation	Yes	No	No	No	No	No
	Seizure Label, Type	Yes, 8	No	No	No	No	No
	No of Channels	19,21	23,24,26	36-100	21	16-72	53-216
Number of Patients and EEGs	Patients	637	24	16	75	12	31
	All EEGs	5,610	683	100	75	12	102
	Non-Seizure EEGs	4,450	545	0	22	0	0
	Seizure EEGs	1,150	138	100	54	12	102
	Seizure Events	3,050	185	100	517	12	102
Duration	All EEGs (in hours)	922	980	13.5	114	7.20	7.96
	Non-SZ EEGs (in hours)	681	792	0	35.0	0	0
	SZ EEGs (in hours)	242	188	13.5	78.6	7.20	7.96
	Average (All) (in minutes)	9.84	86.1	8.1	89.64	36	4.68

Information about the six datasets is summarized in Table 10. We refer to the supplementary notes for more details on the six datasets. The TUH-SZ dataset is the largest among those six datasets, with the most annotated seizure events and eight seizure types (see Supplementary Figure 2). As that dataset contains the most seizure data, we utilize it as the primary source to train the entire seizure detector pipeline. Firstly, the seizure detector is trained and evaluated with the TUH-SZ dataset via 4-fold cross-validation (CV), where we assign approximately the same number of patients and seizures to each of the four-folds. We train the proposed seizure detector on the TUH-SZ dataset, and assess it on the other five independent EEG datasets. In this way, we can examine the generalizability of the detector on different EEG datasets with different EEG types (sEEG and iEEG) and patient age groups (neonates, paediatrics, and adults).

For all the EEGs, a 4th order Butterworth notch filter at 60Hz (USA) and 50Hz (EU) is applied to remove electrical interference⁶⁵. Next, a 1Hz high-pass filter (4th order) is implemented to reject DC shifts and baseline fluctuations⁶⁶. Finally, all the EEGs are downsampled to a sampling frequency F_s of 128Hz. At last, we convert all sEEGs to bipolar montage, as the TUH-SZ dataset is annotated in the bipolar montage. As the montage for the iEEGs is not compatible with the bipolar montage, we keep the montage of the iEEGs at monopolar.

Seizure Detector Pipeline

We perform seizure detection first at individual channels (channel-level detection), next at multi-channel segments (segment-level detection), and at last, we detect the start and end points of the seizures in the entire multi-channel EEG (EEG-level detection)^{65–67} (see Supplementary Figure 1). The pipeline of the proposed seizure detector is displayed in Figure 3. The pipeline consists of a channel-level deep learning classifier, segment-level machine learning classifier, and multiple EEG-level post-processing modules. The seizure detectors are implemented on NVIDIA GeForce GTX1080 GPUs in Keras 2.2.0 and TensorFlow 2.6.0.

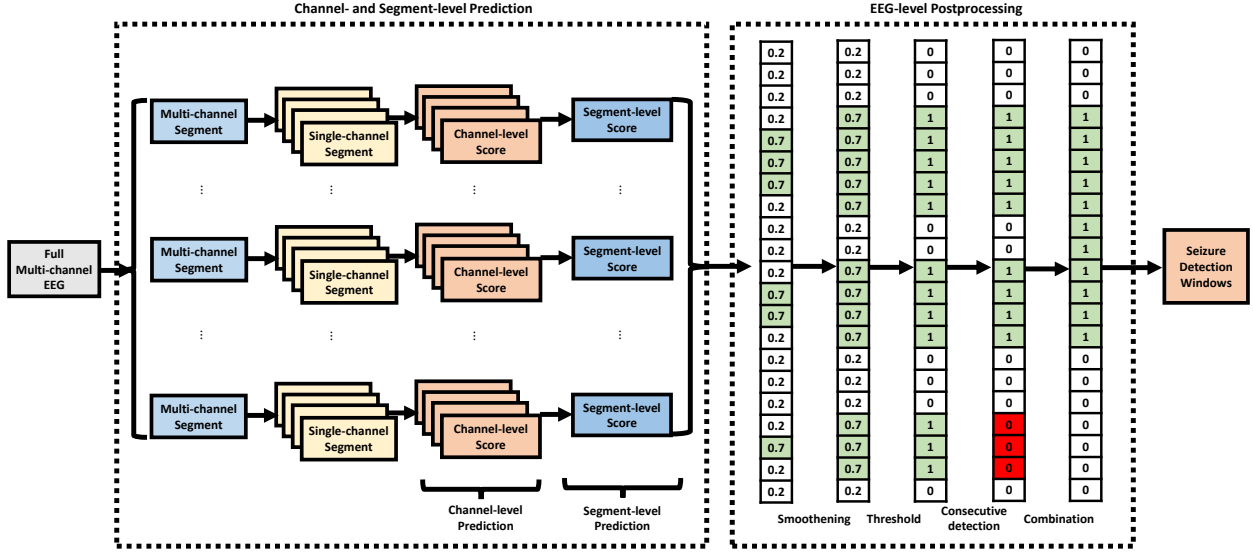


Figure 3. The proposed seizure detector pipeline consists of multiple stages of seizure detection at three EEG scales (channel-level, segment-level, and EEG-level detection). The EEG is divided into overlapping epochs where we performed channel- and segment-level detection to get a series of segment-level predictions. After that, we four postprocessing steps for EEG-level detection. Firstly, we apply smoothing window (max smoothen window of length 3 here) to the segment-level output. Secondly, we implement thresholds (threshold of 0.5 here) to obtain a series of 0s and 1s. Thirdly, we locate chains of consecutive 1s and replace them with 0s if the chain is less than N_c ($N_c = 4$ here) in length. Finally, if any two chains of consecutive 1s are within proximity (3 epochs here), we combine them into a single detection to prevent many fractured detection windows.

Channel-level Seizure Detector

The channel-level seizure detector computes the seizure probability for single-channel EEG segments. For seizure detection, the window length W adopted in the literature ranges between 1s to 30s. However, we believe that 1s is too short to capture long-range seizure morphology, while 30s is too long to capture short seizures. Therefore, we tested window lengths W of 3s, 5s, 10s, and 20s. In this study, we deploy three channel-level seizure detectors based on convolutional neural networks (CNN):

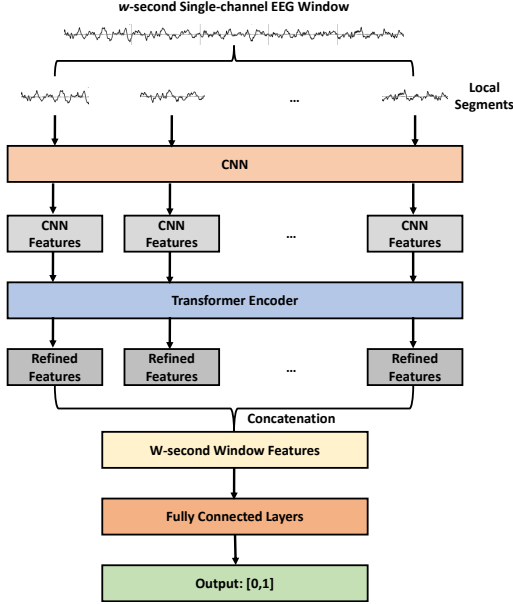
1. CNN with softmax (SM) loss: CNN-SM
2. CNN with belief matching (BM) loss: CNN-BM
3. CNN with transformer and BM loss: CNN-TRF-BM.

CNN-SM Model

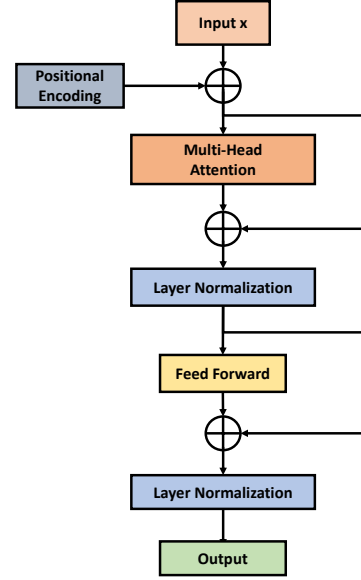
The CNN-SM model is a typical CNN with a SM loss function. The input of the CNN-SM model is the raw single-channel signal of length $W \times F_s$. The CNN architecture contains 5 convolutional layers with 8, 16, 32, 64, and 128 filters, respectively, with two fully connected layers. The architecture is summarized in Supplementary Table 2. To minimize the loss, we applied the Adam optimizer⁶⁸ with an initial learning rate equal to 10^{-4} . The batch size during training is set to 1000. Also, we implemented class weights that are inversely proportional to the class frequency in the training data during training. This allows us to optimize the loss function on an imbalanced dataset without overfitting⁶⁷. Finally, we optimized parameters within the CNN via nested CV on the training data, with an 80:20% split for training and validation.

CNN-BM Model

The CNN-BM model has the same architecture as the CNN-SM model, except that the BM loss replaces the SM loss. Additional details of the BM loss can be found in the supplementary methods. We implemented the BM loss as it has shown to improve uncertainty estimation and calibration compared to the traditional SM loss⁶⁹. Additionally, the BM loss tends to improve generalization performance, which is an important property required for seizure detection.



(a) CNN with transformer encoder.



(b) Transformer encoder.

Figure 4. The architecture of the CNN-TRF-BM model in this study. (a) CNN-TRF-BM model, and (b) transformer encoder.

CNN-TRF-BM Model

The CNN-TRF-BM model contains two components: the CNN and the transformer. The architecture is the same as in the CNN-BM model, but we insert an additional transformer encoder between the final convolutional layer and the flattening layer (see Figure 4(a) and (b)). We implemented a transformer in tandem with the CNN, as the CNN alone cannot model correlations between distant data points, such as seizure morphologies. The transformer can compensate for this limitation by extracting long-range information from the CNN features. The transformer encoder contains eight heads, and the number of hidden layer neurons in the forward feed network (FFN) is 1024. As input to the transformer, we extract 1s segments with 25% overlap from the W -second single-channel segment. More details on the architecture of the transformer can be found in the supplementary methods.

Segment-level Seizure Detector

Next, we rely on the outputs of the channel-level detectors to detect seizures in multi-channel segments. The channel-level detectors yield seizure probabilities for each EEG channel, which we arrange into regions according to the scalp topology: frontal, central, occipital, and parietal. Besides those four local regions, we also define a "global" region containing all channels. From each region, we extract seven statistical features: mean, median, standard deviation, maximum value, minimum value, and value at 25% and 75% percentile. As there are five regions, we extract $5 \times 7 = 35$ features. From all channel-level outputs, we compute the normalized histogram features (5 bins, range set at $[0,1]$), and include them into the feature set, bringing the total features to 40.

In the iEEGs, the channel locations are unavailable. Therefore, we cannot group the iEEG channels into local regions. For consistency, we replace the four local regions with the global region. In this scenario, only 12 features are unique, and the remaining ones are duplicates. In any case, the number of segment-level features is 40, regardless of the total number of channels or the availability of the channel locations. This approach ensures that the number of features is consistent during the training and evaluation of any dataset. The features will be the inputs to a machine learning classifier for training and validation. We employed six machine learning models as candidates for the segment-level classifier: logistic regression (LR), support vector machine (SVM), gradient boosting (GB), AdaBoost (AB), random forest (RF), and XGBoost (XGB). We determined the best model and hyperparameters via grid search CV.

Channel- and Segment-level Evaluation Metric

We assess the channel- and segment-level seizure classifiers through the following metrics: accuracy (ACC), balanced accuracy (BAC), sensitivity (SEN), specificity (SPE), F1 score (F1), and expected calibration error (ECE)⁷⁰. As the seizure and non-seizure classes are imbalanced, we evaluate the results mainly in terms of BAC⁶⁷.

EEG-level Seizure Detector

Finally, we perform seizure detection on full multi-channel EEGs (EEG-level detection). Specifically, we determine the start and end time of the seizures, if any. First, we apply a sliding window of length W with an overlap duration T_o to the multi-channel EEG, extracting n multi-channel segments. The overlap duration T_o is set to 1s. Next, we perform segment-level detection on every segment, resulting in n segment-level seizure probabilities $P = [p_1, \dots, p_n]$. Finally, we conduct three post-processing steps to the seizure probability sequence P :

1. We apply 1D smoothing filters with an overlap of 1 sample. We tested various filter lengths K_f (3s, 5s, or 7s) and filter types (mean, median, and maximum). The smoothing filter removes isolated seizure detections, which are usually false positives (FPs) such as artifacts. Additionally, the filter smoothens regions with large fluctuations (i.e., confidence variations) to stabilize the detections.
2. Next, we perform simple thresholding to the seizure probabilities to round them to zeros (seizure-free) or ones (seizure). We tested threshold values $\theta \in \{0.1, 0.2, \dots, 0.8, 0.9\}$. The resulting sequence will only contain 0s and/or 1s.
3. Then, we identify consecutive ones of length smaller than N_c . If the sequence of ones is shorter than N_c , we replace all the 1s in that sequence with 0s. We tested $N_c \in \{1, 2, \dots, 19, 20\}$ to account for short and long seizures. Selecting a large N_c may lead to fewer FPs, but will create more FNs, as the system will miss out on short seizures.

Finally, we identify the remaining sequences of consecutive ones, and determine their start and end time. However, we must add W -seconds to each end time, as the detector utilized W -seconds after the end time to obtain the final trigger. The final output of the EEG-level seizure detector is the start and end times of the detected seizures.

EEG-level Seizure Detection Evaluation Metric

After collecting all the start and end times of the detected seizures, we assess the accuracy of those detections. There are several well-established evaluation metrics, such as epoch-based sampling (EBS)⁴⁶, any-overlap (OVL)⁴⁶, time-aligned event scoring (TAES)⁴⁶, and increased margin scoring (IMS)¹⁶. However, these metrics do not accurately reflect the requirement of a seizure detector deployed in clinical settings. We elaborate on the limitations of the existing seizure evaluation metrics in the supplementary methods section. In short, OVL metric considers a detection correct as long as it has a non-zero overlap with the annotation, which is too lenient and leads to overly optimistic results. On the other hand, TAES metric is too strict as it requires a perfect overlap between the detection and annotation, leading to overly pessimistic results. Hence, we decided to define a new metric, the minimum overlap evaluation scoring (MOES), that lies between those two extremes. In this metric, there needs to be a non-trivial overlap between the detection and the seizure, while it does not need to be perfect.

Minimum Overlap Evaluation Scoring (MOES)

The minimum overlap evaluation scoring (MOES) determines the overlap duration T_{overlap} between the detection ($T_{\text{detection}} = [d_{\text{start}}, d_{\text{end}}]$) and seizure ($T_{\text{seizure}} = [s_{\text{start}}, s_{\text{end}}]$) window, and vice versa, before deciding if the detection is correct or the seizure is captured. Based on existing literature, only seizures of at least 10s are annotated typically^{71, 72}. Therefore, the minimum overlap duration of the detection(s) with the seizure should be 10s. However, these criteria do not account for the duration of the seizure nor the detection. Even if the detection correctly detected over 10s of a seizure, if the majority of the detection did not capture any seizure, the system should be penalized. To resolve this, we compute the detection overlap (DOL) and the seizure overlap (SOL), which measures the fraction of the detection that overlaps with any seizures, and vice versa, as:

$$\text{DOL}_i = \frac{\sum_s T_{\text{overlap},s,i}}{d_{\text{end},i} - d_{\text{start},i}}, \quad (1)$$

$$\text{SOL}_j = \frac{\sum_d T_{\text{overlap},d,j}}{s_{\text{end},j} - s_{\text{start},j}}, \quad (2)$$

where i and j is the index of a detection and a seizure, respectively, $\sum T_{\text{overlap},s,i}$ is the sum of all the overlaps with any seizures with detection i , and $\sum T_{\text{overlap},d,j}$ is the sum of all the overlaps with any seizures with seizure j .

In this study, we set a minimum DOL and SOL of 0.3 (30%), to ensure that a significant portion of the detection overlaps with the seizures and vice versa. In OVLP metric, the DOL is set to be 0+%, while in TAES it is 100%. The first option is too lenient in practice, while the latter is too strict.

A high DOL implies that the detection overlaps well with the seizure(s). Meanwhile, a high SOL indicates that the seizure is well captured by the detection(s). If the DOL is low, the detection should be discarded and treated as a false positive (FP). Similarly, if the SOL is low, the seizure should be treated as a false negative (FN). This approach allows us to consider different cases (see Figure 5):

- Case 1: The detection window encapsulates the seizure window almost perfectly. Therefore, the $SOL_j = 1$, while $DOL_i > 0.3$ (close to 1). In this case, the seizure_j is a TP as the detection_i is correct.
- Case 2: The detection window is encapsulated by the seizure window almost perfectly. Therefore, the $DOL_i = 1$, while $SOL_j > 0.3$ (close to 1). In this case, the seizure_j is a TP as the detection_i is correct.
- Case 3: The detection window overlaps with the seizure window, however, the detection window protrudes the seizure window by a significant margin. In this case, while the SOL_j can be greater than 0.3, the DOL_i is low (less than 0.3). As $DOL_i < 0.3$, we consider the detection_i as a false alarm (FP). As a result, the seizure_j is considered as a FN.
- Case 4: The seizure window overlaps the detection window, however, the seizure window protrudes the detection window by a significant margin. In this case, while the DOL_i can be greater than 0.3, the SOL_j is low (less than 0.3). As $SOL_j < 0.3$, we consider the seizure_j as missed (FN). As a result, the detection_i is considered as a FP.
- Case 5: Multiple detection windows (1, 2, 3) overlap with the annotated seizure. The majority of the seizure_j is detected, hence the SOL_j is high (greater than 0.3). However, the DOL_i vary for each detection, though all of them clipped the seizure to a certain extent.
 1. Detection₁ would have $DOL_1 \approx 0.5$, hence it is a correct detection.
 2. Detection₂ would have $DOL_2 = 1$, hence it is a correct detection.
 3. Detection₃ would have $DOL_3 < 0.3$, hence it is a false detection.

As $SOL_j > 0.3$, we consider the seizure_j as captured, hence a true positive. Meanwhile, the detection₁ and detection₂ are correct (TP) and detection₃ is considered as a false positive.

- Case 6: Multiple seizure windows (1, 2, 3) overlap with a detection window. The majority of the detection_i had capture seizures, hence the DOL_i is high (greater than 0.3). However, the SOL_j vary for each seizure, though all of them clipped the detection to a certain extent.
 1. Seizure₁ would have $SOL_1 \approx 0.5$, hence the seizure is detected well.
 2. Seizure₂ would have $SOL_2 = 1$, hence the seizure is detected well.
 3. Seizure₃ would have $SOL_3 < 0.3$, hence the seizure is not detected.

As $DOL_i > 0.3$, we consider the detection_j as correct, hence it is not a false positive. Meanwhile, the seizure₁ and seizure₂ are one TP each and detection₃ is missed and is considered as a false negative.

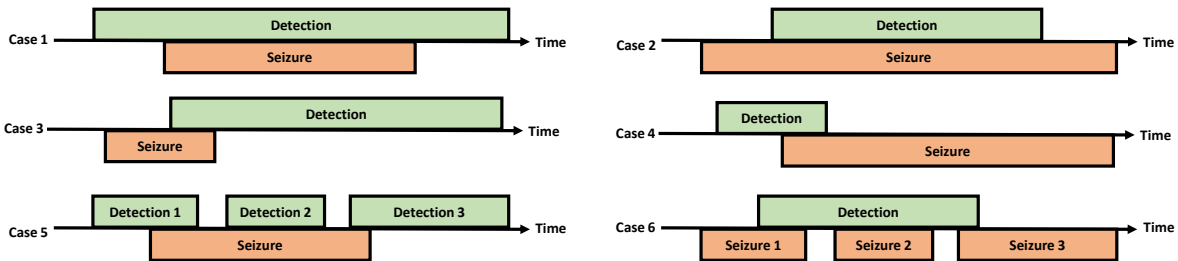


Figure 5. Different cases of seizure detection that may be encountered.

In other words, the detections and seizures are analyzed separately. By investigating the seizures, we can compute the TP. Firstly, we check what detections overlap with the seizure_j. For the seizure to be considered a TP, the following two conditions must be met simultaneously:

1. $SOL_j \geq 0.3$.
2. $DOL_i \geq 0.3$ for all detections overlapping with seizure_j.

The first condition implies that seizure_j is sufficiently captured by one or more detections. The second condition makes sure that each of those detections sufficiently covers a seizure (seizure_j and potentially also other seizures). If both conditions are met simultaneously, the seizure is accurately detected and is a TP. Otherwise, the seizure is missed and it is a FN. Indeed, imagine that 2 detections on the left and right of the seizure last very long and cover together almost the entire EEG. Then the entire EEG is covered by detections, and the seizure would not be properly detected. The two detections could have very low DOL. Consequently, the seizure in that EEG will be considered a FN instead of a TP.

Next, by investigating the detections, we compute the FPs. We first determine what seizures overlap with detection_i. The detection is considered a FP, as long as any of the following two conditions are met:

1. $DOL_i < 0.3$
2. $SOL_j < 0.3$ for all seizures overlapping with detection_i.

Note that it is important to compute TPs from the perspective of the seizure. Indeed, multiple detections may overlap with the same seizure (see Figure 5 Case 6). However, as there is only one seizure event, we only can have one TP or one FN associated with a seizure event. Therefore, we need to compute the TPs from the perspective of the seizures. Computing TP from the perspective of the detection windows may result in multiple TPs for a single seizure event, which is undesirable.

Finally, the detection may start earlier or later than the actual annotation. Hence, one should compute the detection offset. We compute the detection offset as:

$$T_{\text{offset}} = d_{\text{start}} - s_{\text{start}} + W, \quad (3)$$

where W are the duration of the window length, d_{start} is the start time of the detection, s_{start} is the start time of the annotated seizure. We added W in the offset as we require a minimum window of length W to detect seizures. To more accurately detect the onset of a seizure, one may slide the window in smaller steps around the onset of a detection. However, this goes beyond the scope of this work, as we are mainly interested in detecting seizures, irrespective of their onset times.

EEG-level Seizure Detection Performance Metrics

We measure the performance of EEG-level seizure detection by the sensitivity (SEN), precision (PRE), false positive per hour (FPR/h), and median detection offset (in seconds). We report both the average FPR/h (aFPR/h) and median FPR/h (mFPR/h). We mainly focus on the median FPR/h in this study as they are more robust to outliers compared to the average.

References

1. Jirsa, V. K., Stacey, W. C., Quilichini, P. P., Ivanov, A. I. & Bernard, C. On the nature of seizure dynamics. *Brain* **137**, 2210–2230 (2014).
2. Nunes, V. D., Sawyer, L., Neilson, J., Sarri, G. & Cross, J. H. Diagnosis and management of the epilepsies in adults and children: summary of updated nice guidance. *Bmj* **344** (2012).
3. Misulis, K. E. & Murray, E. L. *Essentials of Hospital Neurology* (Oxford University Press, 2017).
4. Britton, J. W. *et al. Electroencephalography (EEG): An introductory text and atlas of normal and abnormal findings in adults, children, and infants* (American Epilepsy Society, Chicago, 2016).
5. Gogou, M. & Cross, J. H. Seizures and epilepsy in childhood. *CONTINUUM: Lifelong Learn. Neurol.* **28**, 428–456 (2022).
6. Rinaldi, V. E., Di Cara, G., Mencaroni, E. & Verrotti, A. Therapeutic options for childhood absence epilepsy. *Pediatr. Reports* **13**, 658–667 (2021).
7. Milán-Tomás, Á., Persyko, M., Del Campo, M., Shapiro, C. M. & Farcnik, K. An overview of psychogenic non-epileptic seizures: etiology, diagnosis and management. *Can. J. Neurol. Sci.* **45**, 130–136 (2018).
8. Organization, W. H. *et al. Atlas: epilepsy care in the world* (World Health Organization, 2005).
9. Ferri, F. F. *Ferri's Clinical Advisor 2020 E-Book: 5 Books in 1* (Elsevier Health Sciences, 2019).

10. Berg, A. T. Risk of recurrence after a first unprovoked seizure. *Epilepsia* **49**, 13–18 (2008).
11. Mormann, F., Andrzejak, R. G., Elger, C. E. & Lehnertz, K. Seizure prediction: the long and winding road. *Brain* **130**, 314–333 (2007).
12. Jayakar, P. *et al.* Diagnostic utility of invasive eeg for epilepsy surgery: indications, modalities, and techniques. *Epilepsia* **57**, 1735–1747 (2016).
13. Geut, I., Weenink, S., Knottnerus, I. & van Putten, M. J. Detecting interictal discharges in first seizure patients: ambulatory eeg or eeg after sleep deprivation? *Seizure* **51**, 52–54 (2017).
14. Sierra-Marcos, A., Scheuer, M. L. & Rossetti, A. O. Seizure detection with automated eeg analysis: a validation study focusing on periodic patterns. *Clin. neurophysiology* **126**, 456–462 (2015).
15. Rommens, N., Geertsema, E., Holleboom, L. J., Cox, F. & Visser, G. Improving staff response to seizures on the epilepsy monitoring unit with online eeg seizure detection algorithms. *Epilepsy & Behav.* **84**, 99–104 (2018).
16. Reus, E., Visser, G., van Dijk, J. & Cox, F. Automated seizure detection in an emu setting: are software packages ready for implementation? *Seizure* (2022).
17. Koren, J., Hafner, S., Feigl, M. & Baumgartner, C. Systematic analysis and comparison of commercial seizure-detection software. *Epilepsia* **62**, 426–438 (2021).
18. Shah, V. *et al.* Optimizing channel selection for seizure detection. In *2017 IEEE Signal Processing in Medicine and Biology Symposium (SPMB)*, 1–5 (IEEE, 2017).
19. Ayodele, K., Ikezogwo, W., Komolafe, M. & Ogunbona, P. Supervised domain generalization for integration of disparate scalp eeg datasets for automatic epileptic seizure detection. *Comput. Biol. Medicine* **120**, 103757 (2020).
20. Chatzichristos, C. *et al.* Epileptic seizure detection in eeg via fusion of multi-view attention-gated u-net deep neural networks. In *Proceedings of the IEEE Signal Processing in Medicine and Biology Symposium (SPMB)*, 7 (2020).
21. Roy, S. *et al.* Evaluation of artificial intelligence systems for assisting neurologists with fast and accurate annotations of scalp electroencephalography data. *EBioMedicine* 103275 (2021).
22. Fürbass, F. *et al.* Prospective multi-center study of an automatic online seizure detection system for epilepsy monitoring units. *Clin. Neurophysiol.* **126**, 1124–1131 (2015).
23. Mansouri, A., Singh, S. P. & Sayood, K. Online eeg seizure detection and localization. *Algorithms* **12**, 176 (2019).
24. Gómez, C. *et al.* Automatic seizure detection based on imaged-eeg signals through fully convolutional networks. *Sci. reports* **10**, 1–13 (2020).
25. Valdez, A. B., Hickman, E. N., Treiman, D. M., Smith, K. A. & Steinmetz, P. N. A statistical method for predicting seizure onset zones from human single-neuron recordings. *J. neural engineering* **10**, 016001 (2012).
26. Soare, I. & Escudero, J. Evaluation of eeg dynamic connectivity around seizure onset with principal component analysis. In *44th Annual International Conference of the IEEE Engineering in Medicine and Biology Society (IEEE Xplore, 2022)*.
27. Ansari, A. H. *et al.* Neonatal seizure detection using deep convolutional neural networks. *Int. journal neural systems* **29**, 1850011 (2019).
28. Yang, Y., Truong, N. D., Maher, C., Nikpour, A. & Kavehei, O. Two-channel epileptic seizure detection with blended multi-time segments electroencephalography spectrogram (2020).
29. Thyagachandran, A., Kumar, M., Sur, M., Aghoram, R. & Murthy, H. Seizure detection using time delay neural networks and lstms. In *2020 IEEE Signal Processing in Medicine and Biology Symposium (SPMB)*, 1–5 (IEEE, 2020).
30. Bhattacharya, A., Baweja, T. & Karri, S. Epileptic seizure prediction using deep transformer model. *Int. J. Neural Syst.* 2150058 (2021).
31. Pedoeem, J., Abittan, S., Yosef, G. B. & Keene, S. Tabs: Transformer based seizure detection. In *2020 IEEE Signal Processing in Medicine and Biology Symposium (SPMB)*, 1–6 (IEEE, 2020).
32. Raghu, S., Sriraam, N., Temel, Y., Rao, S. V. & Kubben, P. L. Eeg based multi-class seizure type classification using convolutional neural network and transfer learning. *Neural Networks* **124**, 202–212 (2020).

33. Saab, K., Dunnmon, J., Ré, C., Rubin, D. & Lee-Messer, C. Weak supervision as an efficient approach for automated seizure detection in electroencephalography. *NPJ digital medicine* **3**, 1–12 (2020).
34. Emami, A. *et al.* Seizure detection by convolutional neural network-based analysis of scalp electroencephalography plot images. *NeuroImage: Clin.* **22**, 101684 (2019).
35. Covert, I. C. *et al.* Temporal graph convolutional networks for automatic seizure detection. In *Machine Learning for Healthcare Conference*, 160–180 (PMLR, 2019).
36. Roy, S., Kiral-Kornek, I. & Harrer, S. Chrononet: a deep recurrent neural network for abnormal eeg identification. In *Conference on Artificial Intelligence in Medicine in Europe*, 47–56 (Springer, 2019).
37. Shellhaas, R. A. & Clancy, R. R. Characterization of neonatal seizures by conventional eeg and single-channel eeg. *Clin. Neurophysiol.* **118**, 2156–2161 (2007).
38. Wusthoff, C., Shellhaas, R. & Clancy, R. Limitations of single-channel eeg on the forehead for neonatal seizure detection. *J. Perinatol.* **29**, 237–242 (2009).
39. Lu, Y., Ma, Y., Chen, C. & Wang, Y. Classification of single-channel eeg signals for epileptic seizures detection based on hybrid features. *Technol. Heal. Care* **26**, 337–346 (2018).
40. Ammar, S. & Senouci, M. Seizure detection with single-channel eeg using extreme learning machine. In *2016 17th international conference on sciences and techniques of automatic control and computer engineering (STA)*, 776–779 (IEEE, 2016).
41. Liu, J. & Woodson, B. Deep learning classification for epilepsy detection using a single channel electroencephalography (eeg). In *Proceedings of the 2019 3rd International Conference on Deep Learning Technologies*, 23–26 (2019).
42. Wang, X. *et al.* One dimensional convolutional neural networks for seizure onset detection using long-term scalp and intracranial eeg. *Neurocomputing* **459**, 212–222 (2021).
43. Henriksen, J. *et al.* Automatic seizure detection: going from seeg to ieeg. In *2010 Annual International Conference of the IEEE Engineering in Medicine and Biology*, 2431–2434 (IEEE, 2010).
44. Zhang, Z. & Parhi, K. K. Low-complexity seizure prediction from ieeg/seeg using spectral power and ratios of spectral power. *IEEE transactions on biomedical circuits systems* **10**, 693–706 (2015).
45. Rout, S. K., Sahani, M., Dash, P. & Biswal, P. K. Multifuse multilayer multikernel rvfln+ of process modes decomposition and approximate entropy data from ieeg/seeg signals for epileptic seizure recognition. *Comput. Biol. Medicine* **132**, 104299 (2021).
46. Ziyabari, S., Shah, V., Golmohammadi, M., Obeid, I. & Picone, J. Objective evaluation metrics for automatic classification of eeg events. *arXiv preprint arXiv:1712.10107* (2017).
47. Cook, M. J. *et al.* Prediction of seizure likelihood with a long-term, implanted seizure advisory system in patients with drug-resistant epilepsy: a first-in-man study. *The Lancet Neurol.* **12**, 563–571 (2013).
48. Burrello, A., Schindler, K., Benini, L. & Rahimi, A. Hyperdimensional computing with local binary patterns: one-shot learning of seizure onset and identification of ictogenic brain regions using short-time ieeg recordings. *IEEE Transactions on Biomed. Eng.* **67**, 601–613 (2019).
49. O’Shea, A., Lightbody, G., Boylan, G. & Temko, A. Neonatal seizure detection from raw multi-channel eeg using a fully convolutional architecture. *Neural Networks* **123**, 12–25 (2020).
50. Brinkmann, B. H. *et al.* Crowdsourcing reproducible seizure forecasting in human and canine epilepsy. *Brain* **139**, 1713–1722 (2016).
51. Shen, Y. Machine learning based epileptic seizure detection for responsive neurostimulator system optimization. In *Journal of Physics: Conference Series*, vol. 1453, 012089 (IOP Publishing, 2020).
52. Li, A. *et al.* Neural fragility as an eeg marker of the seizure onset zone. *bioRxiv* 862797 (2021).
53. Cox, F., Reus, E., Widman, G., Zwemmer, J. & Visser, G. Epilepsy monitoring units can be safe places; a prospective study in a large cohort. *Epilepsy & Behav.* **102**, 106718 (2020).
54. Asif, U., Roy, S., Tang, J. & Harrer, S. Seizurenet: Multi-spectral deep feature learning for seizure type classification. In *Machine Learning in Clinical Neuroimaging and Radiogenomics in Neuro-oncology*, 77–87 (Springer, 2020).

55. Hossain, M. S., Amin, S. U., Alsulaiman, M. & Muhammad, G. Applying deep learning for epilepsy seizure detection and brain mapping visualization. *ACM Transactions on Multimed. Comput. Commun. Appl. (TOMM)* **15**, 1–17 (2019).
56. Yuan, Y., Xun, G., Jia, K. & Zhang, A. A multi-view deep learning framework for eeg seizure detection. *IEEE journal biomedical health informatics* **23**, 83–94 (2018).
57. Zhou, M. *et al.* Epileptic seizure detection based on eeg signals and cnn. *Front. neuroinformatics* **12**, 95 (2018).
58. Khalkhali, V. *et al.* Low latency real-time seizure detection using transfer deep learning. In *2021 IEEE Signal Processing in Medicine and Biology Symposium (SPMB)*, 1–7 (IEEE, 2021).
59. Shah, V. *Improved Segmentation for Automated Seizure Detection Using Channel-Dependent Posteriors* (Temple University, 2021).
60. Peh, W. Y., Yao, Y. & Dauwels, J. Transformer convolutional neural networks for automated artifact detection in scalp eeg. *arXiv preprint arXiv:2208.02405* (2022).
61. Shah, V. *et al.* The temple university hospital seizure detection corpus. *Front. neuroinformatics* **12**, 83 (2018).
62. Shoeb, A. *et al.* Patient-specific seizure onset detection. *Epilepsy & Behav.* **5**, 483–498 (2004).
63. Stevenson, N., Tapani, K., Lauronen, L. & Vanhatalo, S. A dataset of neonatal eeg recordings with seizure annotations. *Sci. data* **6**, 1–8 (2019).
64. Wagenaar, J. B., Brinkmann, B. H., Ives, Z., Worrell, G. A. & Litt, B. A multimodal platform for cloud-based collaborative research. In *2013 6th international IEEE/EMBS conference on neural engineering (NER)*, 1386–1389 (IEEE, 2013).
65. Thomas, J. *et al.* Automated adult epilepsy diagnostic tool based on interictal scalp electroencephalogram characteristics: A six-center study. *Int. J. Neural Syst.* 2050074 (2021).
66. Thangavel, P. *et al.* Time–frequency decomposition of scalp electroencephalograms improves deep learning-based epilepsy diagnosis. *Int. J. Neural Syst.* 2150032 (2021).
67. Peh, W. Y. *et al.* Multi-center validation study of automated classification of pathological slowing in adult scalp electroencephalograms via frequency features. *Int. J. Neural Syst.* 2150016 (2021).
68. Kingma, D. P. & Ba, J. Adam: A method for stochastic optimization. *arXiv preprint arXiv:1412.6980* (2014).
69. Joo, T., Chung, U. & Seo, M.-G. Being bayesian about categorical probability. In *International Conference on Machine Learning*, 4950–4961 (PMLR, 2020).
70. Guo, C., Pleiss, G., Sun, Y. & Weinberger, K. Q. On calibration of modern neural networks. In *International Conference on Machine Learning*, 1321–1330 (PMLR, 2017).
71. Afra, P., Jouny, C. C. & Bergey, G. K. Duration of complex partial seizures: an intracranial eeg study. *Epilepsia* **49**, 677–684 (2008).
72. Krystal, A. D. *et al.* Comparison of seizure duration, ictal eeg, and cognitive effects of ketamine and methohexital anesthesia with ect. *The J. neuropsychiatry clinical neurosciences* **15**, 27–34 (2003).

Author contributions statement

J.D. and W.Y.P. conceived and designed the experiments, W.Y.P. T.P., and Y.Y.Y. conducted the experiments, W.Y.P., J.D., T.P., J.T., and Y.L.T. analyzed and discussed the results. J.D. and W.Y.P. wrote the manuscript. All authors provided critical feedback and helped shape the research, analysis and manuscript.